Final response to the referees' comments for Olin et al.: "Contribution of traffic-originated nanoparticle emissions to regional and local aerosol levels"

We thank the referees for their insightful comments and have corrected the manuscript according to them.

Referee reports are in *black italic* and authors' responses in blue roman font. **Bold blue** or ~~struck-through blue~~ fonts highlight changed text parts in some comments. The marked-up manuscript and the Supplement highlighting the changes are included at the end of this file.

Referee comment 1 (anonymous):

1. *Olin et al. introduce an interesting study on how aerosol particle number emissions described with a previous inventory can be improved by implementing newer emission factor data. The authors derive emission factors for traffic in different size bins from their observations, apply these to improve the description of emissions in an air quality model, estimate the composition of the particles in different size ranges, compare the original and updated modelled particle size distributions and compositions with observations, and discuss the improvements of the update in terms of human health impacts. The topic is timely and the results are interesting and would deserve to be published in ACP, but in the current version the description of the methods and stepwise presentation of results is not adequate for fully understanding the results.*

2. *I list first my major comments related to the methods and their illustration, and below this, more detailed comments related to the text. If the authors can satisfactorily reply to these comments and modify the manuscript accordingly, I can recommend the publication in ACP.*

Major comments:

3. *The authors do not present any figures on the determination of EFPSD, which is one corner stone of this study. They refer to their earlier study in which a similar method was applied for sub-3 nm particles. However, I would assume that the determination of emission factors for larger particles is not as simple, due to their longer lifetimes which causes more varying back-ground concentrations. Where one can expect that sub-3 nm particles at the kerbside are fresh particles either from the traffic or from NPF, larger particles may originate from sources further away and their concentration can be expected to be less sensitive to nearby sources, especially with time resolution as low as 9 minutes. The authors also conclude that the derived EFPSD agrees with the one reported by Hietikko et al. (2018) and that this implies the method used in this article is acceptable. To evaluate the acceptability, the reviewers and the readers need to see how the data look like.*

Figure FR1 presents examples of determining EFs for three different particle size bins (geometric mean diameters of 1.9, 16, and 55 nm). The lowest one corresponds to sub-3 nm particles. It can be seen that linear behavior of the particle concentrations against the CO_2 concentrations is observed both for the sub-3 nm particles and for the larger particles too. Longer lifetimes of larger particles can cause that they are originated not from the studied street but from a larger area, such as from the nearby streets or from the whole urban area. Nevertheless, the linear behavior proves that there are particles which can be connected to traffic emissions, although they might not be originated from the studied street. Fig. FR1 is now added to the Supplement (Fig. S1) and the following text to the manuscript:

"Whereas NCA measured at the curbside probably originates from the studied street or via atmospheric NPF, larger particles—having longer atmospheric lifetime—can be originated also from larger area, including nearby streets or the whole urban area. Nevertheless, due to the fact that linear fitting of the particle concentrations from every size bin against the CO_2 concentration is possible (Fig. S1), their relation to the traffic is evident, although all particle sizes may not be originated from the studied street."

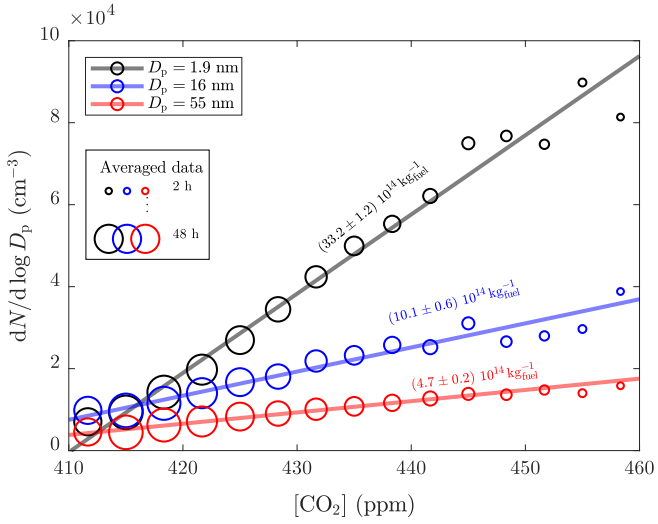

Figure FR1. Examples of determining emission factors bin-by-bin for three different particle size bins, similarly to the method by Olin et al. (2020). Size-binned particle number concentration data ($\mathrm{d}N/\mathrm{d}\log D_\mathrm{p}$) are averaged within CO_2 concentration ($[CO_2]$) bins (circle diameters represent the amount of data used in the averaging). Linear fitting (using the circle diameters as weighting factor) is performed over the averaged data (separately for all 28 measured size bins). The slopes of the linear fits converted to kilograms of fuel combusted are marked in the figure.

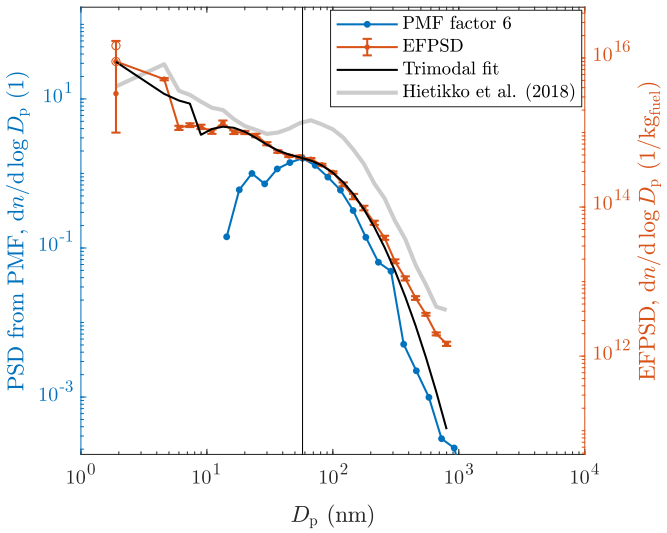

Figure FR2. The shape of the difference PSD measured at Mäkelänkatu (Hietikko et al., 2018) added for comparison (the data is scaled so that it can be easily compared with the EFPSD data).

For better evaluation of the acceptability of deriving an EFPSD from the measured PSDs, the difference PSD (background PSD subtracted from the PSD measured when wind blew from the road) from Hietikko et al. (2018) is now added to Fig. 1 (shown here in Fig. FR2).

4. *The authors use PMF on the diurnal patterns of the EUCAARI emission inventory to extract the contribution of traffic. Does the detailed category-level specification of emissions not exist anymore? Have the producers of the emission data (Denier van der Gon and others at TNO) been contacted to inquire for such specification? If they have been contacted and the specification does not exist, this should be clearly stated and the personal communication to TNO could be used as a reference. Otherwise, I would strongly recommend the authors to reconsider making this contact. The study would seem much more exact or accurate if the original traffic emission output data could be applied.*

We agree that the original traffic emission data would be more exact and accurate. However, we were forced to extract the spatial and temporal patterns and the binned particle emissions and their compositions using the PMF approach because they are not available separately for different source categories, neither at least openly nor at least without significant reprocessing steps by experts not involved in this project. TNO has been contacted. The sentence "Due to the unavailability of the emission rates in a source category-level, updating only road transport-related emissions was not straightforward." is now replaced with the sentence "Because the particle number emission rates **in 41 size bins** in a source category-level were not **openly** available, updating only road transport-related emissions was not straightforward." to highlight the need for the binned emissions and the availability of the original emissions.

Nevertheless, we were able to compare the PMF factor 6 (considered here the road traffic-related source) to the road traffic-related source of the original inventory as the total particle mass emission rates because they were available in a source category-level for the inventory too. Figure FR3 presents the comparison as maps and diurnal variations. It can be seen that the spatial (maps) and temporal (diurnal variations) patterns agree well, with some exceptions, such as some ship routes and slightly higher rates with the PMF factor 6. Therefore, the PMF approach does not cause significant errors to the simulation results.

This discussion is now included in the manuscript (Sec. 3.2.1), Fig. FR3 is now added to the Supplement, and the map and diurnal variation figures (Fig. S2 and S3) in the Supplement are now updated to mass-based variables. Additionally, the map and diurnal variation plot are now removed from Fig. 1 because they are now compared with Fig. FR3 in the Supplement.

5. *The authors use CFD modelling for determining the composition of European wide aerosol emissions from traffic. If I understood correct, this CFD model result is based on one diesel bus. Since the CFD model is described only in (non-peer reviewed) MSc thesis (in Finnish), the description of the model and main results should be given in the article. Part of this could be included in the supplementary material. The composition results are not compared to any previous article and the composition is not discussed in the introduction. In the current form, the part on composition should not be published in ACP.*

CFD-modelling was used for determining the chemical composition of particles emitted by road traffic due to a scarcity of related studies, especially when considering particles smaller than 50 nm, which are inefficiently detected with, e.g., an aerosol mass spectrometer. In this first level approximation for updating the road traffic-emitted PSD using a single PSD for the whole European vehicle fleet as in the case of the original inventory as well, the composition was also approximated using a single composition for the whole fleet although it is based on a diesel-fueled bus only. This assumption is now further discussed (and found reasonable) in the manuscript using results from other related studies with the following paragraph added to Sec. 3.2.4:

"The selection of the CFD-simulations of a diesel-fueled bus for determining chemical composition of particles was further elaborated by examining other related studies as well. Kostenidou et al. (2021) measured chemical composition of particles emitted by different gasoline- and diesel-fueled Euro 5 light-duty vehicles over different transient driving cycles on a dynamometer. Calculated from the reported EFs, the mass fractions of BC, SO_4, and POA in the total aerosol were 0.58–0.98, 0.00–0.30, and 0.02–0.15, respectively. Similarly, Pirjola et al. (2019) measured a diesel-fueled Euro 4 light-duty vehicle and reported the BC, SO_4, and POA mass fractions of 0.81–0.88, 0.00–0.03, and 0.11–0.18, respectively. These mentioned mass fractions are comparable to the mass fractions in the soot mode from the CFD-simulations (Table 1). However, it should be noted that in the mentioned studies, SO_4, and POA were measured using aerosol mass spectrometers, which do not efficiently

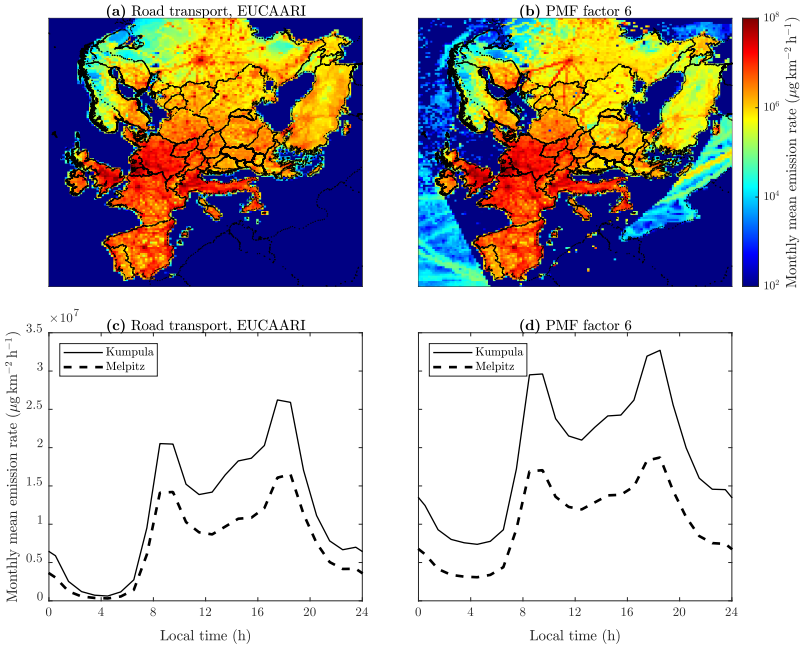

Figure FR3. Monthly means of the particle mass emission rates (**a**,**c**) from the road transport-related source in the original EUCAARI inventory and (**b**,**d**) from PMF factor 6 (**a**,**b**) as maps and (**c**,**d**) as diurnal variations in Kumpula/Mäkelänkatu, Finland, and Melpitz, Germany.

detect particles smaller than ~ 50 nm. Therefore, the composition of the nucleation mode, or especially of the power law mode, is barely covered in the measured compositions and studies related to these compositions are very scarce. According to the formation principle of nucleation mode particles, they do not contain BC; thus, POA dominates in the mass fractions of the nucleation mode (Table 1) as it dominates in the mass fractions of the volatile (SO_4 and POA) part of the soot mode. Hao et al. (2019) collected PM2.5 particle samples on filters from a highway tunnel in China and reported the BC, SO_4, and POA mass fractions of 0.12, 0.09, and 0.34, respectively. These values lie in the range between the mass fractions of the nucleation and soot modes from the CFD-simulations. In conclusion, due to the scarcity of studies on chemical composition of vehicle-emitted particles and because the CFD-simulated mass fractions (of a diesel bus only) are reasonable according to the other studies (including tailpipe emissions of both gasoline- and diesel-fueled light-duty vehicles and emissions from a real traffic mixture from a road tunnel), the CFD-simulated ones were used here to cover the whole vehicle fleet. In addition, this study primarily focuses on the updating of the shape of the PSD, but not on the exact chemical composition of emitted particles, which was, however, required to be estimated for running the model with the updated inventory."

The sentence:

"Because measuring chemical composition for sub-50 nm particles is challenging, this study relies on CFD-simulations of particle composition 10 m behind a diesel-fueled bus by Olin (2013)."

in the preceding paragraph is also now replaced with the sentences:

"To add particles to the original road transport-related PSD, a selection for their chemical composition was needed. Because measuring chemical composition for sub-50 nm particles is challenging, this study relies on CFD-simulations of particle composition 10 m behind a diesel-fueled bus by Olin (2013). They consist of a situation where a Euro III bus is driving at a speed of 40 km/h with the engine power of 40 % of the maximum (see the Supplement for a more detailed description)."

and the Supplement now includes a section "Description of the CFD-simulations used to determine chemical composition of the emitted particles", in which the basics and the applied results of the CFD-simulations are described.

Composition is not discussed in the introduction because it is not of the main interest of this study.

Minor comments:

6. *Lines 33-34: Traffic emissions in Paasonen et al (2016) are not based on EUCAARI inventory, but on EU FP7 project TRANSPHORM.*

That's true. The text is now updated to read: "Paasonen et al. (2016) estimated future projections of particle number concentrations in a global scale using emission inputs based **partially** on the same inventory**, but, e.g., traffic emissions based on the EU FP7 project TRANSPHORM database (Vouitsis et al., 2013)**.

7. *Lines 80-85: is the composition of diesel bus exhaust assumed for the whole fleet? Some words about how this assumption may bias the results.*

Please refer to the answer of the comment 5.

8. *Line 92: Some words about how the interpolation may bias the results. Why not using simply 9 min averages of CO2 as well?*

Interpolation of the DMPS data to 1 min time resolution was used because other data was in 1 min resolution too. However, we tested the other method too: keeping the DMPS data in 9 min resolution and averaging the CO_2 data to 9 min resolution. This did not have significant differences on the obtained EFPSD: values were slightly ($\sim 6\,\%$) higher but the uncertainties were at least 2-fold compared to the interpolation method. Therefore, we selected the interpolation method.

The sentence:

"The PSDs measured with the DMPS in 9 min time resolution were interpolated to 1 min resolution before calculating the EFs."

is now updated to read:

"To express all data in similar time resolution, the PSDs measured with the DMPS in 9 min resolution were interpolated to 1 min resolution before calculating the EFs."

9. *Lines 100-103: some references to the observation sites should be included.*

The reference to the article by Kulmala et al. (2011) is now added as the reference for the EUSAAR stations.

10. *Line 106: Could refer to recent Okuljar et al. article.*

The reference to the article by Okuljar et al. (2021) is now added to this sentence.

11. *Lines 145-155: Why do you not investigate further factors 7 and 11, which both seem to be related to rush hours? How is their size distribution and is there a good reason to exclude them? At least factor 7 would contribute significantly to overall result.*

It is true that also the factor 11 seems to be related to rush hours, but it was omitted due to its PSD (Fig. FR4) and map features. Maps and diurnal variation plots are now expressed in mass-based variables, instead of number-based variables, because they are now compared to the ones from the road traffic-related source of the original inventory (Fig. FR3), which is available as the total particle mass emission rate.

The factor 7 was also omitted due to its PSD and because the factor 6 seems to be enough to represent the whole road transport-source category (seen as slightly higher values in Fig. FR3d).

This discussion is now included in the manuscript (Sec. 3.2.1), Figs. FR4 and FR3 are now added to the Supplement, and the map and diurnal variation figures (Fig. S2 and S3) in the Supplement are now updated to mass-based variables.

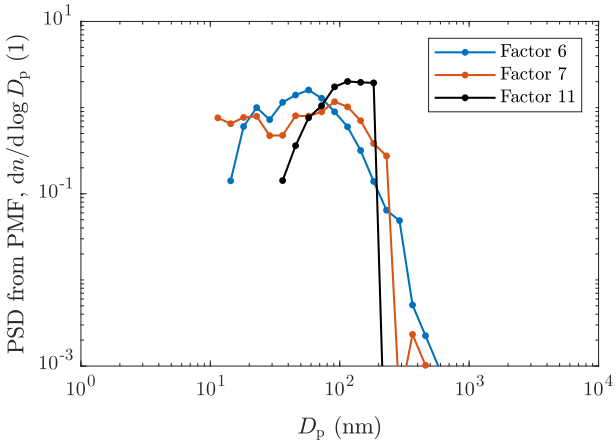

Figure FR4. Particle size distributions obtained from PMF factors 6, 7, and 11.

12. *Line 148: Since the Denier van der Gon -report is not available without request from the project office, the count mean diameter and/or other features of their PSD should be listed.*

It is now mentioned in the manuscript that "the on-road diesel exhaust PSD, presented by Denier van der Gon et al. (2009)" is "a bimodal distribution having the modes at 23 and 57 nm".

13. *Line 176: Luoma et al seem to have the trend calculated mainly for periods 2015-2019. They also mention that the applied trend, -7.1 %/a for PM2.5, is the only trend they could not determine a statistically significant trend. Can you somehow justify extending similar trend to 2008?*

Although statistically not a significant trend, the trend for PM2.5 was applied because the primary objective was to scale the soot modes onto the same levels. In this way, we were able to consider only updating of the shape of the emitted PSD and to omit the updating of the level of emissions overall. This is now clarified in the manuscript; additionally, an estimation of the realism of the trend of $-7.1\,\%\mathrm{a}^{-1}$, using the trend of the concentration of 56 nm-sized particles measured in Kumpula between years 2008 and 2017 and the trend of road transport-emitted PM2.5 in Finland reported by EMEP (2021) for years between 2008 and 2017, is now added.

The following text is now added to Sec. 3.2.2:

"The yearly decrease rate of PM2.5 ($7.1\,\%\mathrm{a}^{-1}$) was, however, reported as statistically not a significant trend (Luoma et al., 2021) and also it only covers the trend between years 2015 and 2018. Thus, a trend was also estimated with the data from Kumpula, which fully cover the years between 2008 and 2017. Applying a seasonal Mann-Kendall test and Sen's slope estimator—as done by Luoma et al. (2021)—to the particle number concentration at 56 nm, measured by a DMPS in Kumpula, gives the yearly decrease rate of $4.4\,\%\mathrm{a}^{-1}$ for the years between 2008 and 2017. Since this trend is for Kumpula, the trend for Mäkelänkatu could be around $7.1\,\%\mathrm{a}^{-1}$ because the trends of other quantities for Mäkelänkatu were found to be approximately 2-fold than for Kumpula in the study by Luoma et al. (2021). Additionally, the PM2.5 trend was calculated from the data of yearly (1990–2019) road transport emissions (without road, tyre, and brake wear) in Finland, reported by EMEP (2021). The decreasing trend calculated for the years between 2008 and 2017 is $6.0\,\%\mathrm{a}^{-1}$, which corresponds relatively well to the trend applied here ($7.1\,\%\mathrm{a}^{-1}$)."

and the following text to Sec. 3.2.3:

"Nevertheless, the scaling of the soot modes was a primary objective here because, hence, the update of the inventory considers only updating the shape of the emitted PSD (below 57 nm), but not its level overall."

14. *Lines 216-218: While this is possibly the case, this sentence should be reconsidered when the Paasonen et al. (2016) paper is notified to be updated in terms of traffic emissions from EUCAARI to TRANSPHORM. One way to discuss the representativeness of Paasonen et al. emissions may be to reflect their comparison to emission size distribution calculated from long-term observations in Kontkanen et al. (2020, https://doi.org/10.5194/acp-20-11329-2020).*

The suggested discussion is now added to the manuscript with the following text after the sentence in question:

"Emissions of sub-10 nm particles have been applied also in the study by Paasonen et al. (2016), who included a size bin for 3–10 nm particles, based on the TRANSPHORM database (Vouitsis et al., 2013). However, they did not include any modes smaller than 10 nm; thus, this size bin was only an extension from PSDs with larger modes. Kontkanen et al. (2020) compared annual size-binned particle emissions between their estimations from ambient data measured in urban Beijing and the model by Paasonen et al. (2016). They observed that the ambient data suggest significantly more particles in sub-60 nm size range. This is due to the fact that the ambient data represent emissions from a more localized—traffic-influenced—area but also because the smallest particles are omitted from the traffic emissions in the TRANSPHORM database."

15. *Lines 220-227: An equation including the three different modes, or at least better explanation, should be given. I am not entirely sure if I understand what the trimodal fit here means. The authors often refer to previous studies in a way that even basic understanding of what is done in this study is not possible to get without reading the other articles (same holds for the determination of emission factor, see my first major comment).*

We agree that some useful detailed information were missing in the manuscript. This issue of understanding of the trimodal fitting is now clarified by adding a note "(see the Supplement for the detailed equation)" to the text and by adding the detailed equation to the Supplement.

16. *Lines 228-232: Would be good to mention here also that PMF 6 is presumably related to diesel particles only. And that NCA emissions are not described for other sources in EUCAARI inventory.*

That's a good idea. Not only NCA emissions are described only for road transport in the updated inventory, but actually all sub-10 nm particles. The paragraph is now updated to:

"The contribution of the road transport-related particle number emissions (from the PMF factor 6**, which is presumably related only to diesel vehicles**) to the total emissions from ~~the~~ all emission sources was averagely 8 % in the original inventory. In updating the inventory, the**se** road transport-related particle number emissions were increased to a 26-fold level, resulting in the increase of the total number emissions to a 3-fold level. Hence, in the updated inventory, the contribution of the**se** road transport-related particle number emissions **(from diesel vehicles)** to the total emissions becomes 69 %. **Due to the lack of all sub-10 nm particle emissions in the original EUCAARI inventory, sub-10 nm particle emissions in the updated one come exclusively from road transport.**"

17. *Line 275: Some references required for the underestimation of PSD measurements in sub-10 nm size range.*

A reference to the article by Kangasluoma et al. (2020) is now added in this sentence. Additionally, the reference to the article by Olin et al. (2019) in a sentence also on the underestimation of PSD measurements on line 48 is now replaced with the reference to the article by Kangasluoma et al. (2020), representing a wider study on device comparison in sub-10 nm size range.

18. *Line 281-282. It would be interesting to see separate figures for the different sites, especially to those where one would expect the traffic emissions to play a big role in <10 nm concentrations (Kumpula and possibly Melpitz).*

The following sentence is now added to the caption of Fig. 3:

"See Fig. S6 for a clearer presentation of the data from the stations with the highest traffic influences only (Melpitz and Kumpula)."

and Fig. FR5 is now added to the Supplement. From this new figure, the stations with the highest traffic influences only (Melpitz and Kumpula) are more clearly distinguished.

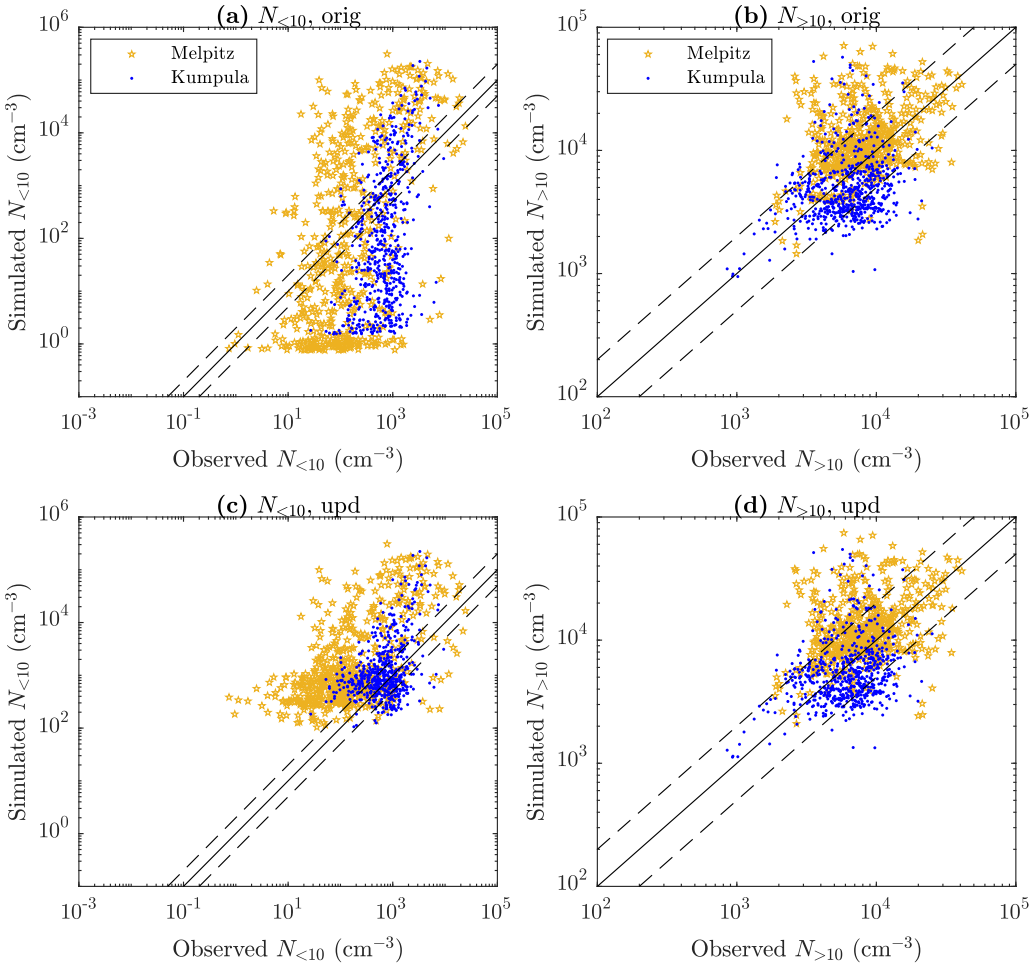

Figure FR5. Simulated versus observed number concentrations of particles (**a**, **c**) smaller than 10 nm ($N_{<10}$) and (**b**, **d**) larger than 10 nm ($N_{>10}$) at the stations with the highest traffic influences (Melpitz and Kumpula) with (**a**, **b**) the original and (**c**, **d**) updated emission inventory. All data correspond to hourly means for May 2008. The solid diagonal lines represent 1:1 lines and the dashed ones 1:2 and 2:1 lines.

19. *Lines 290-293: Increasing condensation sink is a plausible reason for decreasing modelled concentrations, but do you have any evidence of that being the reason? N>100 does not seem to change (Table 2), but how much does N>50 change? Or could you draw a map of change in coagulation sink as well? Also later, in Fig. 7, it is difficult to understand the difference in sink: Fig 7c shows very similar size distribution for original and updated model run in sizes >30nm, actually with higher concentration in original run in 40-50 nm and 500-600 nm size ranges. It looks like the sink in the original run in 7c is higher than in the updated run, whereas the interpretation of the differences in lines 341-343 suggests the opposite.*

It is very likely that increased condensation and coagulation sinks affect the concentrations via decreased NPF rates so that the concentrations also decrease after updating the inventory. There is an evidence of at least NPF being connected to the decreasing concentrations: by simulating with the NPF processes switched off, updating the inventory only increases the concentrations. This discussion (including coagulation sink mentioned) is now included in the manuscript by replacing the text:

"This results via increased primary emissions of particles increasing the condensation sink, which can reduce nucleating gaseous precursors and thus lead to lowered NPF rates. Due to a complex relationship between the increase of the condensation sink and the decrease of the NPF rate, updating the emission inventory can change the particle concentrations in both directions."

with the text:

"This results via increased primary emissions of particles increasing the condensation **and coagulation** sink**s**, which can reduce nucleating gaseous precursors **and newly formed particles, respectively,** and thus lead to **less small particles**. Due to a complex relationship between the increase**s** of the sink**s** and the **appearance of small particles**, updating the emission inventory can change the particle concentrations in both directions. **It is clear that decreased concentrations are related to the connection between NPF and emissions because simulating with NPF processes switched off results in the situation in which updating the inventory only increases the concentrations.**"

and by mentioning coagulation sink too in the discussion of Fig. 7 and in the conclusions.

As the change in the values for $N_{>100}$ with updating the inventory in Table 2, the change in $N_{>50}$ is also minor. It should be noted that those values correspond to the data from the selected measurement stations for the whole month, but the decreasing concentration effect is better observed when examining in shorter timescales. Figure FR6 illustrates the maps for the ratios of monthly means of the condensation and coagulation sinks. By comparing these maps to the maps in Fig. 5, it can be observed that the sinks become higher mainly over the ground, in average, but there are several areas with decreased concentrations over the seas. Because higher concentrations basically lead to higher sinks, the increased sinks and the decreased concentrations are not seen at the same areas in averaged maps. This highlights that the effect of adding more particle emissions can lead to decreased concentrations too is a phenomenon which occurs within large areas.

The case in Fig. 7 does actually have $\sim 4\,\%$ lower condensation sink with the updated inventory as you interpreted. The concentrations decreased with the updated inventory because the condensation (and coagulation) sink has become higher during the previous time steps. Thus, nucleating precursors could have depleted beforehand so that the total NPF rate has become to the level of only one third of the rate simulated with the original inventory and thus giving lower concentrations for the time range in question. Additionally, the neighboring grid cells have even higher sinks; thus, the effect can also be transported from nearby areas. This discussion is now included in the manuscript with the following text added after the discussion of Fig. 7:

"However, the sinks are actually $\sim 4\,\%$ lower with the updated inventory during the time range presented in Fig. 7. Instead, the sinks just before the time range were $\sim 6\,\%$ higher and even $\sim 10\,\%$ higher in an adjacent grid cell. The effect of increased sinks with the updated inventory on the appearance of small particles is not always observed within a single time step or grid cell but within later time steps or nearby grid cells instead, due to a history effect and transportation of components between the grid cells."

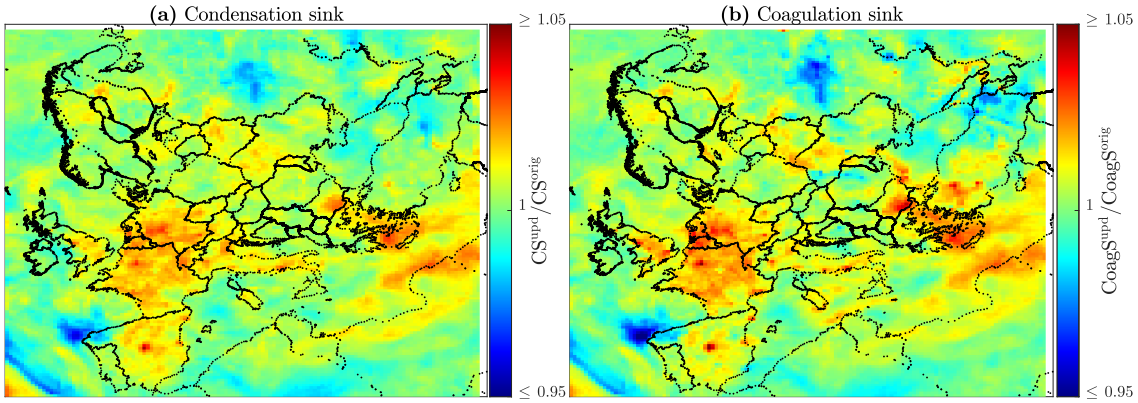

Figure FR6. Ratios of monthly means of (**a**) the condensation sink (CS) and (**b**) the coagulation sink (CoagS) simulated with the updated and with the original emission inventory.

20. *Additionally, related to Fig 7c, I wonder why the modelled PSD jumps so much up and down between different size ranges: the difference in concentrations in neighbouring size bins can be up to two orders of magnitude and the nucleation, Aitken and accumulation mode do not show any modal distribution. Also in Fig 6., the modelled size distributions are surprisingly unsmooth for monthly means.*

The model has internally a tendency to output PSDs in which concentrations in adjacent size bins are clearly different. For better readability, Figs. 6, 7, and 8 are now reproduced using smoothing from the adjacent bins. Nucleation, Aitken, and accumulation modes are also seen more clearly now, especially in Fig. 7c.

21. *Lines 355-356: Is the line for observations in London missing, or are there no observations? Why wouldn't the authors use Kumpula observations instead or additionally to London as an example of site with traffic in vicinity? London is not even mentioned in Section 2.2. If there is no data from London, adding Kumpula (or Melpitz) data becomes even more crucial.*

Although there are no suitable observational data for London, it was selected because it was a good example of high traffic densities and low NPF rates (during mornings). It's a good suggestion to use a location for which observational data are available instead of London. Therefore, the data for London in Fig. 8a is now replaced with the data corresponding to Melpitz (the observed distribution is also shown), where similar effects to London are seen too. Melpitz was selected due to high traffic densities nearby. Kumpula would not be as good example because it is located in a grid cell including also sea areas and because photochemical activity—and thus NPF—begins earlier in May due to its northerner location.

22. *Language overall: There are many quite long and difficult sentences, due to which I suggest the authors to doublecheck the language in general. Additionally, the use of the word "unity" instead of "one" or "one-to-one" in "ratio over or below unity" does not sound good to me. In my understanding unity is something that cannot be exceeded.*

The language has now been doublechecked. Several long sentences are now revised and split into multiple sentences. The words "unity" are now replaced using the words "one".

Referee comment 2 (Hugo Denier van der Gon):

23. *The study describes an elegant empirical way to update the only European size-resolved Particle Number inventory and evaluates the results against observations .Ultra fine particles (UFP) and particle numbers (PN) in the atmosphere are not regulated like PM2.5 or PM10. There are no air quality limit values nor obligations to monitor these metrics. As a result our understanding, emission data, measurements, concentrations and related information is scarce. Clearly more information is needed and the paper is a welcome and original contribution, and fitting for ACP. In my opinion the paper can be published after some corrections and further clarifications have been made.*

Major points

24. *In the introduction first & second paragraph it would be good to already stress/explain that the EUCAARI inventory by definition considers only particles > 10 nm. The reason being that for many emission sources size-resolved PN measurements are extremely scarce, and EFs for <10 nm are either non-existent or highly variable. Literature is also often not clear about the cut-off. To have a more robust result the EUCAARI inventory was made for size bins of 10 nm and up. However, as pointed pout by the authors, this does not mean that the PN , 10 nm are not important and it is very relevant to investigate this. Therefore "updating" mostly means extending the range of the inventory to include an important but difficult size range.*

The second paragraph is now updated to include the sentence:

"Only emissions of particles larger than 10 nm were estimated in the EUCAARI inventory, because emissions of especially sub-10 nm particles for many emission sources have not been determined with high enough certainty or not determined at all."

25. *It is also suggested to explain a bit better that the road transport regulation for PN > 23 nm for non-volatile PN was chosen to have a reproducible measurement. For a standard this is a great advantage. However, a large part of the emitted PN are volatile and it is questionable if this standard for non-volatile PN > 23 nm has any relation or even correlation with the real world total (volatile + non-volatile) size -resolved PN emissions. This relates also to L 301 where some remarks are made about "unregulated vehicle -emitted particles" but volatile particles > 23 nm are also unregulated. So, that is not well-defined in the MS because it suggests road transport particles > 23 nm are regulated but it is only a fraction of these.*

This is now explained better in the introduction by replacing the text:

"...the fact that only non-volatile particles larger than 23 nm are currently regulated in number emission standards (Giechaskiel et al., 2012) and that the emission factors (EFs) of the smallest particles are quite variable across the vehicle fleet. A high level of variation is caused by the nature of the nucleation process—the main origin of the smallest particles at least in diesel exhaust—which is very sensitive to several factors..."

with the text:

"...the fact that only non-volatile particles larger than 23 nm have been selected as the regulated ones in current road transport number emission standards (Giechaskiel et al., 2012) because measuring them is far more reproducible than of volatile ones. Many of the components of the smallest particles do, however, evaporate when heated. Hence, there are also emissions of particles larger than 23 nm (volatile ones) which are currently unregulated. The emission factors (EFs) of the smallest particles are quite variable across the vehicle fleet due to the nature of the nucleation process—their main origin at least in diesel exhaust—which is very sensitive to several factors..."

The text at the line 301 is also updated to "$N_{<23}$ (**totally** unregulated vehicle-emitted particles, $D_\mathrm{p} < 23\,\mathrm{nm}$)" to clarify that the sub-23 nm particles are totally unregulated (both volatile and non-volatile parts).

26. *Somewhere in the introduction explain more clearly why you choose to do simulations for a year (2008) that is by now 12-13 years in the past. It is not trivial. Many things have changed by now especially in road transport but also e.g. shipping with fuel sulphur regulations.*

Simulations were done for May 2008 because this period has become a kind of a standard period for PMCAMx-UF simulations for the European domain and is thus used in many other studies as well. Therefore, the model inputs for emissions and meteorology were directly available for that period already. The end part of the introduction is now updated to:

"The simulated period **(May 2008)** was photochemically relatively active, which elevates NPF to the major source of new particles. **This period was chosen because the same period has been simulated in several other related studies as well, providing plenty of comparable data and pre-defined input files for emissions and meteorology. Since the street canyon measurements were performed in 2017—using more recent technologies for PSD measurements—trends of urban aerosol and vehicle emissions were used to scale the determined emissions from 2017 to 2008.**"

27. *L186 The updating process was stopped at 57 nm, meaning no changes for Dp > 57 nm. Many studies investigate ultrafine particles which are defined as < 100 nm. Although not the subject of study it would be good to state in discussion or conclusion what the impact of the update is for anthropogenic UFP emissions, especially for road transport. How much does UFP increase? This may help to put in perspective with other studies.*

The impacts of the update for the road transport-related emissions and for the total emissions, in respect to UFP number, are now calculated and included in the text in Sec. 3.2.4 with the following sentence:

"By considering only the number concentrations of ultrafine particles (UFP, sub-100 nm particles), the road transport-related emissions were increased to a 28-fold level. This resulted in that the total UFP number emissions were increased by a factor of 3.1."

Table S1, representing the ratios of monthly means of concentrations simulated with the updated and with the original inventory, is now updated to include also the ratios for the number concentration of UFPs ($N_{<100}$). Whereas the mean increase was $0.9\,\%$ for the total particle number, it was $1.1\,\%$ for the UFP number.

28. *L190 – why was the scaling done using measurements from 2015 onwards. It would also be possible to use the trend in reported PM2.5 emissions from Finland for road transport exhaust (available at https://www.ceip.at/). Does that give different results? Or do you have a motivation why that would not work?*

Although not covering the years between 2008 and 2015, the trend for PM2.5 was applied because the primary objective was to scale the soot modes onto the same levels. In this way, we were able to consider only updating of the shape of the emitted PSD and to omit the updating of the level of emissions overall. This is now clarified in the manuscript; additionally, an estimation of the realism of the trend of $-7.1\,\%\mathrm{a}^{-1}$, using the trend of the concentration of 56 nm-sized particles measured in Kumpula between years 2008 and 2017 and the trend of road transport-emitted PM2.5 in Finland reported by EMEP (2021) for years between 2008 and 2017, is now added.

The following text is now added to Sec. 3.2.2:

"The yearly decrease rate of PM2.5 ($7.1\,\%\mathrm{a}^{-1}$) was, however, reported as statistically not a significant trend (Luoma et al., 2021) and also it only covers the trend between years 2015 and 2018. Thus, a trend was also estimated with the data from Kumpula, which fully cover the years between 2008 and 2017. Applying a seasonal Mann-Kendall test and Sen's slope estimator—as done by Luoma et al. (2021)—to the particle number concentration at 56 nm gives the yearly decrease rate of $4.4\,\%\mathrm{a}^{-1}$ for the years between 2008 and 2017. Since this trend is for Kumpula, the trend for Mäkelänkatu could be around $7.1\,\%\mathrm{a}^{-1}$ because the trends of other quantities for Mäkelänkatu were found to be approximately 2-fold than for Kumpula in the study by Luoma et al. (2021). Additionally, the PM2.5 trend was calculated from the data of yearly (1990–2019) road transport emissions (without road, tyre, and brake wear) in Finland, reported by EMEP (2021). The decreasing trend calculated for the years between 2008 and 2017 is $6.0\,\%\mathrm{a}^{-1}$, which corresponds relatively well to the trend applied here ($7.1\,\%\mathrm{a}^{-1}$)."

and the following text to Sec. 3.2.3:

"Nevertheless, the scaling of the soot modes was a primary objective here because, hence, the update of the inventory considers only updating the shape of the emitted PSD (below 57 nm), but not its level overall."

29. *In the conclusions e.g. around L 415 it would be important to stress / mention that road transport is not the only anthropogenic source where such an update (adding the smaller particles) would havean impact. I would expect that for aviation (airports close to a city) and shipping (in the case of port cities) this would further increase the PN emissions. You do not have to add these emission here but it is good to mention that this should be addressed as well. How would further addition influence your model results? Is there room for this or would it lead to overestimating?*

It is possible—and even likely—that other anthropogenic sources, such as aviation and shipping activities, may involve underestimations of small particles similar to road transport due to similar reasons. There also seems to be room for adding particle emissions for those activities because, e.g., measured PSDs are higher than the simulated ones for Kumpula, which is located near ($< 15\,\mathrm{km}$) a busy airport and harbor areas. The following text is now added to Sec. 3.3.3:

"Additionally, there are a busy airport and harbor areas within a radius of 15 km from the Kumpula station. It is certainly possible that, in addition to road transport, other activities, such as aviation and shipping, can also involve underestimated particle emissions. Hence, other anthropogenic particle emission sources may also need to be addressed better in emission inventories, in order to have the simulated PSDs to agree with the measured ones."

and the following sentence to the last paragraph of the manuscript:

"In addition to road transport, other anthropogenic emission sources, such as aviation and shipping activities, may need to be addressed better in emission inventories, because they may involve underestimated particle emissions as well."

30. *L 345 and further: Do you think having substantial sub-10 nm BC particles is realistic? As BC is a product of incomplete combustion it seems not very likely to me? You state it could also be other non-volatile components such as metals but if that is the case, isn't it better to call it non-volatile instead of BC?*

We agree that soot particles are usually larger than 10 nm. Because the composition of sub-10 nm particles are quite unknown and because we did not want to add an extra component to the inventory (would have required several modifications to the model code), we decided to lump the non-volatile part together with BC. This is now better explained in the text and BC in the updated inventory is now called BC*. Calling it "non-volatile" would not be the best option because there are also other components in the inventory which are non-volatile. The following sentence in Sec. 3.2.4:

"The non-volatile part is here assumed to be BC due to the lack of more specific information."

is now replaced with the sentences:

"The non-volatile part is here lumped together with BC due to the lack of more specific information on its composition and because adding an extra component would have required several modifications to the model code. BC together with the unknown non-volatile part is abbreviated here to BC*."

and the "BC*" abbreviations are now added into legends of Figs. 2b and 7a,d. Also the discussion related to Fig. 7 in Sec. 3.3.4 is now updated to include the "BC*" abbreviations.

31. *Moreover & related, I find this "based on results from one diesel bus" (L82) rather tricky in the light of the whole study. How representative is one Finnish diesel bus for the whole European fleet? Why do the authors feel that is good enough? I think this needs better discussion and motivation.*

Please refer to comment 5 (from the another referee) and our reply to it (begins on page 3 of this document) which is a similar comment to this one.

Minor points / corrections

32. *L38 regulated in* ***road transport*** *emission standards [it is better to be specific here]*

The text:
"only non-volatile particles larger than 23 nm are currently regulated in number emission standards"
is now changed to (partially due to comment 25):
"only non-volatile particles larger than 23 nm have been selected as the regulated ones in current road transport number emission standards"

33. *L80 composition of NCA - easier for the reader to have "composition of 1-3 nm sized particles"*

We decided to keep the form "the composition of NCA (volatile and non-volatile fractions)" there because the form "composition of 1-3 nm sized particles (volatile and non-volatile fractions)" could be more easily mixed with chemical composition, which is not the case here. The word "composition" here refers to the fractions of volatile and non-volatile parts of NCA.

34. *L82 chemical composition "obtained from a computational fluid dynamics (CFD) simulation" I find that hard to understand. How can you obtain chemical composition from a CFD simulation? Can you rewrite / explain a bit better?*

It is actually an aerosol dynamics model which gives the chemical composition for particles. This model was coupled with a CFD model. This is now explained better with the updated text: "obtained from **a simulation with an aerosol dynamics model coupled with** a computational fluid dynamics (CFD) ~~simulation~~ **model**"

35. *L143 for ~~the~~ both*

The word "the" is now removed from the sentence.

36. *L170 and further: The CO2 trick is transparent and elegant but some more discussion or caution on how reliable it is to scale that way to 2008.*

It is true that scaling the emission factors, determined from the data from 2017, to year 2008 needs caution because CO_2 emissions from road transport have decreased during the years. Determining the EFs using the CO_2 concentrations gives the EFs with respect to kilograms of fuel combusted. Thus, they are applicable to any year. However, the model requires the emission input as time-based particle emission rates. The total amount of fuel combusted has been higher in 2008 than in 2017. Therefore, the emission input would need scaling upwards from year 2017 to year 2008. However, this scaling has already been performed when the EFs were scaled using the trends of PM2.5, because ambient PM2.5 concentrations have decreased not only due to equipping vehicles with a DPF but also due to the fact that the total amount of fuel combusted has decreased. Hence, the scaling of different levels of CO_2 emissions has been performed internally already. This discussion is now included in the text with the following paragraph in Sec. 3.2.2:
"Because fuel efficiency has developed during the years, CO_2 emissions from road transport have been on different levels in 2008 and in 2017. The method of determining EFs using CO_2 concentrations gives the EFPSD with respect to kilograms of fuel combusted. Therefore, it can be applied to any year. However, the total amount of combusted fuel in the computational grid with respect to time has changed, leading to the need of scaling the time-based particle emission rates—which is the form of the emission input of the model—upwards from year 2017 to year 2008. This scaling has, however, already been performed when the EFs were scaled using the trends of PM2.5, because ambient PM2.5 concentrations have decreased not only due to equipping vehicles with a DPF but also due to the fact that the total amount of fuel combusted has decreased."

37. *L174 " the EF of PM2.5 has probably been higher in 2008."Not probably but certainly – you can check the EEA/EMEP emission inventory guidebook for EFs for different EURO classes.*

The text is now updated to: "the EF of PM2.5 has ~~probably~~ been higher in 2008 **(EMEP, 2021)**.".

38. *L 178 is **the** same*

The word "the" is now added into this sentence.

39. *L202 – I am not sure how reassuring the "European average" is . This will be mixing e.g. the UK, Sweden, Bulgaria, Portugal etc. The average may not be very representative of what is seen in the different countries if fleet ages and dominant fuel types are highly variable. On average they may cancel out but PN exposure is about the local urban emissions not about the average emission.*

This is now discussed in Sec. 3.2.3 with the following added text:

"It should, however, be noted that averaging of vehicle ages or fuel types over Europe is not the most representative in terms of the average emissions or particle exposure because there are countries having old vehicle fleet with mostly diesel vehicles—a combination with a plenty of soot emissions—but also countries having new vehicle fleet also with mostly diesel vehicles—a combination with the least particle emissions. In addition, there are countries with other possible mixtures of fleet ages and fuel types of vehicles as well."

40. *Table 1 – Table top row - Please add the size range behind Nucleation and Soot. Easier for the reader.*

We decided to keep the table in its current form because the table already includes count median diameters (CMD) of the nucleation and soot mode (the size range from D_1 to D_2 for the power law mode). Because the nucleation and soot modes are log-normal distributions, there are, by definition, no lower and upper limits of their particle sizes (except 0.8 nm and 10 µm of the PMCAMx-UF model itself).

41. *L229 from the all*

The word "the" is now removed from this sentence as it was probably actually meant with "the".

42. *Table 2 – caption "(the more intended one being bold)." This is cryptic – please rewrite e.g. you mean the best performing in bold?*

Yes, "the best performing" was supposed to be meant. It now reads "(the best performing in bold)".

43. *L 304 so that ~~the~~ half*

The word "the" is now removed from the sentence.

44. *L335 the lie on the range = lie in the range*

The word "on" is now replaced with the word "in" in this sentence.

45. *L336 – please rewrite – "travel to human body" is wrong /strange*

The text "can travel to human body" is now replaced with "can thus end up in human body".

46. *L 366 after ~~the~~ updating*

The word "the" is now removed from the sentence.

47. *L384 "previously underestimated emissions of sub-50 nm particles" I would say "previously partly excluded or partly non-estimated emissions of sub-50 nm particles " The EUCAARI inventory had on purpose a cut-off at 10 nm. In that way it was not "underestimated" but simply not estimated.*

The text is now updated to: "previously ~~understimated~~ **partly excluded** emissions of sub-50 nm particles".

48. *L386 "The reason for the overestimations may be related to overestimated new particle formation" Don't you think that must be related is better? Because the model runs with the original inventory do not include any anthropogenic particles < 10 nm but still give the overestimation?.*

The overestimation may be related to overestimated NPF, but not exactly must be because there is still a possibility that NPF is estimated correctly but the PSD measurements give too low concentrations. Nevertheless, it is sure that the underestimations of sub-10 nm particles are not caused by overestimating their emissions because the overestimations were observed also using the original inventory, in which all sub-10 nm particle emissions were excluded. Additionally, there is a possibility that NPF is estimated correctly but the particle growth out of sub-10 nm size range is underestimated, which was discussed in Sec. 3.3.1 but not in this concluding section. This discussion is now included in the concluding section with the following updated text:

"The reason for the overestimations may be related to overestimated new particle formation (NPF) **or underestimated particle growth** but also to possibly underestimated particle concentrations from the PSD measurements, which are known to become inaccurate for particle sizes below ∼10 nm. **At least, the overestimations of sub-10 nm particles using the updated inventory are not caused by overestimating their emissions because the overestimations were observed also using the original inventory, in which all sub-10 nm particle emissions were excluded.**"

49. *L391 – cryptic – please rewrite*

There was a sentence missing from this text, causing a confusing text. The missing sentence is now added and the following text:

"There are locations and times having the ratios over and below unity while the mean and median values were slightly over unity. This denotes that the predicted concentrations were increased or decreased with a factor of up to several thousands, depending on the examined particle size range, in certain locations and at certain times after updating the inventory."

is also updated to finally read:

"Ratios of simulated particle concentrations after and before updating the inventory were examined from daily and monthly means of local concentrations. The ratios over and below one were observed while the mean and median values were slightly over one: the predicted concentrations were increased or decreased with a factor of up to several thousands, depending on the examined particle size range, in certain locations and at certain times after updating the inventory."

50. *L396 total **anthropogenic** particle number (or is that not the case?)*

The word "anthropogenic" is now added to this sentence.

51. *L405 replace fuel-combusting vehicles with combustion processes – I don't think the fact that it is a vehicle is important.*

The words "fuel-combusting vehicles" are now replaced with the words "combustion processes" in this sentence.

52. *L413 whenever = provided*

This sentence is now updated to read: "The used model can be operated with a grid resolution of down to, e.g., 1 km^2, ~~whenever~~ **provided that** an emission inventory for that resolution is available."

References

Denier van der Gon, H. A. C., Visschedijk, A. J. H., Johansson, C., Hedberg Larsson, E., Harrison, R., and Beddows, D.: Size-resolved pan European anthropogenic particle number inventory, EUCAARI Deliverable report D141 (available on request from EUCAARI project office), 2009.

EMEP: Centre on Emission Inventories and Projections (CEIP): Officially reported emission data, last access: 2 October 2021, available at: https://www.ceip.at/, 2021.

Giechaskiel, B., Mamakos, A., Andersson, J., Dilara, P., Martini, G., Schindler, W., and Bergmann, A.: Measurement of Automotive Nonvolatile Particle Number Emissions within the European Legislative Framework: A Review, Aerosol Sci. Tech., 46, 719–749, https://doi.org/10.1080/02786826.2012.661103, 2012.

Hao, Y., Deng, S., Yang, Y., Song, W., Tong, H., and Qiu, Z.: Chemical Composition of Particulate Matter from Traffic Emissions in a Road Tunnel in Xi'an, China, Aerosol Air Qual. Res., 19, 234–246, https://doi.org/10.4209/aaqr.2018.04.0131, 2019.

Hietikko, R., Kuuluvainen, H., Harrison, R. M., Portin, H., Timonen, H., Niemi, J. V., and Rönkkö, T.: Diurnal variation of nanocluster aerosol concentrations and emission factors in a street canyon, Atmos. Environ., 189, 98–106, https://doi.org/10.1016/j.atmosenv.2018.06.031, 2018.

Kangasluoma, J., Cai, R., Jiang, J., Deng, C., Stolzenburg, D., Ahonen, L. R., Chan, T., Fu, Y., Kim, C., Laurila, T. M., Zhou, Y., Dada, L., Sulo, J., Flagan, R. C., Kulmala, M., Petäjä, T., and Lehtipalo, K.: Overview of measurements and current instrumentation for 1–10 nm aerosol particle number size distributions, J. Aerosol Sci., 148, 105 584, https://doi.org/10.1016/j.jaerosci.2020.105584, 2020.

Kontkanen, J., Deng, C., Fu, Y., Dada, L., Zhou, Y., Cai, J., Daellenbach, K. R., Hakala, S., Kokkonen, T. V., Lin, Z., Liu, Y., Wang, Y., Yan, C., Petäjä, T., Jiang, J., Kulmala, M., and Paasonen, P.: Size-resolved particle number emissions in Beijing determined from measured particle size distributions, Atmos. Chem. Physics, 20, 11 329–11 348, https://doi.org/10.5194/acp-20-11329-2020, 2020.

Kostenidou, E., Martinez-Valiente, A., R'Mili, B., Marques, B., Temime-Roussel, B., Durand, A., André, M., Liu, Y., Louis, C., Vansevenant, B., Ferry, D., Laffon, C., Parent, P., and D'Anna, B.: Technical note: Emission factors, chemical composition, and morphology of particles emitted from Euro 5 diesel and gasoline light-duty vehicles during transient cycles, Atmos. Chem. Phys., 21, 4779–4796, https://doi.org/10.5194/acp-21-4779-2021, 2021.

Kulmala, M., Asmi, A., Lappalainen, H. K., Baltensperger, U., Brenguier, J.-L., Facchini, M. C., Hansson, H.-C., Hov, Ø., O'Dowd, C. D., Pöschl, U., Wiedensohler, A., Boers, R., Boucher, O., de Leeuw, G., Denier van der Gon, H. A. C., Feichter, J., Krejci, R., Laj, P., Lihavainen, H., Lohmann, U., McFiggans, G., Mentel, T., Pilinis, C., Riipinen, I., Schulz, M., Stohl, A., Swietlicki, E., Vignati, E., Alves, C., Amann, M., Ammann, M., Arabas, S., Artaxo, P., Baars, H., Beddows, D. C. S., Bergström, R., Beukes, J. P., Bilde, M., Burkhart, J. F., Canonaco, F., Clegg, S. L., Coe, H., Crumeyrolle, S., D'Anna, B., Decesari, S., Gilardoni, S., Fischer, M., Fjaeraa, A. M., Fountoukis, C., George, C., Gomes, L., Halloran, P., Hamburger, T., Harrison, R. M., Herrmann, H., Hoffmann, T., Hoose, C., Hu, M., Hyvärinen, A., Hõrrak, U., Iinuma, Y., Iversen, T., Josipovic, M., Kanakidou, M., Kiendler-Scharr, A., Kirkevåg, A., Kiss, G., Klimont, Z., Kolmonen, P., Komppula, M., Kristjánsson, J.-E., Laakso, L., Laaksonen, A., Labonnote, L., Lanz, V. A., Lehtinen, K. E. J., Rizzo, L. V., Makkonen, R., Manninen, H. E., McMeeking, G., Merikanto, J., Minikin, A., Mirme, S., Morgan, W. T., Nemitz, E., O'Donnell, D., Panwar, T. S., Pawlowska, H., Petzold, A., Pienaar, J. J., Pio, C., Plass-Duelmer, C., Prévôt, A. S. H., Pryor, S., Reddington, C. L., Roberts, G., Rosenfeld, D., Schwarz, J., Seland, Ø., Sellegri, K., Shen, X. J., Shiraiwa, M., Siebert, H., Sierau, B., Simpson, D., Sun, J. Y., Topping, D., Tunved, P., Vaattovaara, P., Vakkari, V., Veefkind, J. P., Visschedijk, A., Vuollekoski, H., Vuolo, R., Wehner, B., Wildt, J., Woodward, S., Worsnop, D. R., van Zadelhoff, G.-J., Zardini, A. A., Zhang, K., van Zyl, P. G., Kerminen, V.-M., S Carslaw, K., and Pandis, S. N.: General overview: European Integrated project on Aerosol Cloud Climate and Air Quality interactions (EUCAARI) – integrating aerosol research from nano to global scales, Atmos. Chem. Phys., 11, 13 061–13 143, https://doi.org/10.5194/acp-11-13061-2011, 2011.

Luoma, K., Niemi, J. V., Aurela, M., Fung, P. L., Helin, A., Hussein, T., Kangas, L., Kousa, A., Rönkkö, T., Timonen, H., Virkkula, A., and Petäjä, T.: Spatiotemporal variation and trends in equivalent black carbon in the Helsinki metropolitan area in Finland, Atmos. Chem. Phys., 21, 1173–1189, https://doi.org/10.5194/acp-21-1173-2021, 2021.

Okuljar, M., Kuuluvainen, H., Kontkanen, J., Garmash, O., Olin, M., Niemi, J. V., Timonen, H., Kangasluoma, J., Tham, Y. J., Baalbaki, R., Sipilä, M., Salo, L., Lintusaari, H., Portin, H., Teinilä, K., Aurela, M., Dal Maso, M., Rönkkö, T., Petäjä, T., and Paasonen, P.: Measurement report: The influence of traffic and new particle formation on the size distribution of 1–800 nm particles in Helsinki – a street canyon and an urban background station comparison, Atmos. Chem. Phys., 21, 9931–9953, https://doi.org/10.5194/acp-21-9931-2021, 2021.

Olin, M.: Dieselpakokaasun hiukkaspäästöjen muodostumisprosessin simulointi, M.Sc. thesis, Tampere University of Technology, Tampere, Finland, http://urn.fi/URN:NBN:fi:tty-201312191517, 2013.

Olin, M., Alanen, J., Palmroth, M. R. T., Rönkkö, T., and Dal Maso, M.: Inversely modeling homogeneous $H_2SO_4-H_2O$ nucleation rate in exhaust-related conditions, Atmos. Chem. Phys., 19, 6367–6388, https://doi.org/10.5194/acp-19-6367-2019, 2019.

Olin, M., Kuuluvainen, H., Aurela, M., Kalliokoski, J., Kuittinen, N., Isotalo, M., Timonen, H. J., Niemi, J. V., Rönkkö, T., and Dal Maso, M.: Traffic-originated nanocluster emission exceeds H_2SO_4-driven photochemical new particle formation in an urban area, Atmos. Chem. Phys., 20, 1–13, https://doi.org/10.5194/acp-20-1-2020, 2020.

Paasonen, P., Kupiainen, K., Klimont, Z., Visschedijk, A., Denier van der Gon, H. A. C., and Amann, M.: Continental anthropogenic primary particle number emissions, Atmos. Chem. Phys., 16, 6823–6840, https://doi.org/10.5194/acp-16-6823-2016, 2016.

Pirjola, L., Kuuluvainen, H., Timonen, H., Saarikoski, S., Teinilä, K., Salo, L., Datta, A., Simonen, P., Karjalainen, P., Kulmala, K., and Rönkkö, T.: Potential of renewable fuel to reduce diesel exhaust particle emissions, Appl. Energ., 254, 113 636, https://doi.org/https://doi.org/10.1016/j.apenergy.2019.113636, 2019.

Vouitsis, I., Ntziachristos, L., and Samaras, Z.: Methodology for the quantification of road transport PM emissions, using emission factors or profiles, TRANSPHORM Deliverable D1.1.2, http://transphorm.nilu.no/Portals/51/Documents/Deliverables/NewDeliverables/D1.1.2_updated.pdf, 2013.

Contribution of traffic-originated nanoparticle emissions to regional and local aerosol levels

Miska Olin[1], David Patoulias[2,3], Heino Kuuluvainen[1], Jarkko V. Niemi[4], Topi Rönkkö[1], Spyros N. Pandis[2,3], Ilona Riipinen[5], and Miikka Dal Maso[1]

[1]Aerosol Physics Laboratory, Tampere University, FI-33014 Tampere, Finland
[2]Department of Chemical Engineering, University of Patras, GR-26504 Patras, Greece
[3]Institute of Chemical Engineering Sciences, Foundation for Research and Technology, GR-26504 Patras, Greece
[4]Helsinki Region Environmental Services Authority (HSY), FI-00066 HSY, Finland
[5]Department of Environmental Science (ACES) and Bolin Centre for Climate Research, Stockholm University, SE-10691 Stockholm, Sweden

Correspondence: Miska Olin (miska.olin@tuni.fi)

Abstract. Sub-50 nm particles originating from traffic emissions pose risks to human health due to their high lung deposition efficiency and potentially harmful chemical composition. We present a modelling study using an updated EUCAARI number emission inventory, incorporating a more realistic, empirically justified particle size distribution (PSD) for sub-50 nm particles from road traffic as compared with the previous version. We present experimental PSDs and CO_2 concentrations, measured in a highly trafficked street canyon in Helsinki, Finland, as an emission factor particle size distribution (EFPSD), which was then used in updating the EUCAARI inventory. We applied the updated inventory in a simulation using the regional chemical transport model PMCAMx-UF over Europe for May ~~2008~~ 2008. This was done to test the effect of updated emissions in regional and local scales~~and in contrast to~~ , particularly in comparison with atmospheric new particle formation (NPF). Updating the inventory increased the simulated average total particle number concentrations by only 1 %, although the total particle number emissions were increased to a 3-fold level. The concentrations increased up to 11 % when only 1.3–3 nm-sized particles (nanocluster aerosol, NCA) were considered. These values indicate that the effect of updating overall is insignificant in a regional scale during this photochemically active period~~, during which~~ . During this period, the fraction of the total particle number originating ~~through~~ from atmospheric NPF processes was 91 %~~. These~~ ; thus, these simulations give a lower limit for the contribution of traffic to the aerosol levels. Nevertheless, the situation is different when examining the effect of the update closer spatially or temporally, or when focusing to the chemical composition or the origin of the particles. For example, the daily average NCA concentrations increased by a factor of several hundreds or thousands in some locations on certain days. Overall, the most significant effects—reaching several orders of magnitude—from updating the inventory are observed when examining specific particle sizes (especially 7–20 nm), particle components, and specific urban areas. While the model still has a tendency to predict more sub-50 nm particles compared to the observations, the most notable underestimations in the concentrations of sub-10 nm particles are ~~, after updating, overcomeand~~ now overcome. Additionally, the simulated distributions now agree better with the data observed at locations having high traffic densities. The findings of this study highlight the need to consider emissions, PSDs, and composition of sub-50 nm particles from road traffic in studies focusing on urban air quality.

Updating this emission source brings the simulated aerosol levels particularly in urban locations closer to observations, which highlights its importance for calculations of human exposure to nanoparticles.

1 Introduction

Detailed emission inventories are necessary for predictions of air quality and atmospheric composition in general. At present, very few of the standard inventories focus in enough detail on particle number concentrations and size distributions of particles from various sources. Several modelling studies using the regional chemical transport model PMCAMx-UF (Jung et al., 2010) over Europe (Fountoukis et al., 2012; Ahlm et al., 2013; Baranizadeh et al., 2016; Julin et al., 2018; Patoulias et al., 2018) have relied on the pan-European particle number emission (Denier van der Gon et al., 2009; Kulmala et al., 2011) and carbonaceous aerosol (Kulmala et al., 2011) inventories developed in the EUCAARI (European Aerosol Cloud Climate and Air Quality Interactions) project (the combination of these inventories is referred here as the EUCAARI inventory). The EUCAARI inventory includes emissions from electricity production, industry, road and non-road transport, waste disposal, and agriculture. Paasonen et al. (2016) estimated future projections of particle number concentrations in a global scale using emission inputs based partially on the same inventory, but, e.g., traffic emissions based on the EU FP7 project TRANSPHORM database (Vouitsis et al., 2013).

While road transport is a significant particle source in areas affected by vehicles, such as in urban environments (Shi et al., 2001; Kumar et al., 2014), the EUCAARI inventory, however, does not fully consider the traffic-originated emissions of the smallest (especially sub-50 nm, in diameter, D_{p}) particles. This results partially from the fact that only non-volatile particles larger than 23 nm ~~are currently regulated in~~ have been selected as the regulated ones in current road transport number emission standards (Giechaskiel et al., 2012) ~~and that the~~ because measuring them is far more reproducible than of volatile ones. Many of the components of the smallest particles do, however, evaporate when heated. Hence, there are also emissions of particles larger than 23 nm (volatile ones) which are currently unregulated. The emission factors (EFs) of the smallest particles are quite variable across the vehicle fleet ~~. A high level of variation is caused by~~ due to the nature of the nucleation process—~~the main origin of the smallest particles~~ their main origin at least in diesel exhaust—which is very sensitive to several factors, e.g., fuel properties, driving parameters, exhaust after-treatment technology, and environmental parameters (Keskinen and Rönkkö, 2010). ~~These small particles are typically seen~~ Only emissions of particles larger than 10 nm were estimated in the EUCAARI inventory, because emissions of especially sub-10 nm particles for many emission sources have not been determined with high enough certainty or not determined at all.

Particles formed via a nucleation process are typically observed as a different mode—called nucleation mode—in the particle size distribution (PSD) of the exhaust. Although the nucleation mode particles are formed from primary gaseous emissions after the exhaust is released from the exhaust pipe, they are modeled similarly to primary emissions in regional or global models because the grid sizes can be kilometers but the nucleation processes occurring in exhaust plumes occur in scales of a few meters at most. In addition to the high level of variation in the concentrations of the smallest particles in vehicle exhaust, PSD measurements with differential mobility particle sizer (DMPS) or scanning mobility particle sizer (SMPS) typically

underestimate the concentrations in sub-10 nm size range ~~(Olin et al., 2019)~~(Kangasluoma et al., 2020). Furthermore, particles smaller than 3 nm have remained undetected until ~~the~~ recent advances of measurement techniques, such as the introduction of the particle size magnifier (PSM), which is capable of detecting particles down to ∼1 nm (Vanhanen et al., 2011). Traffic has recently been shown to be a major source of those previously undetected particles (nanocluster aerosol, NCA) in traffic-influenced areas (Rönkkö et al., 2017).

Sub-50 nm or sub-23 nm particles originating from traffic are not negligible in terms of human health effects: they have higher deposition efficiency in the human respiratory system as compared with larger particles, and can translocate even to the brain (Oberdörster et al., 2004). They also overlap with the sizes of particles formed and grown during atmospheric new particle formation (NPF) events, and have therefore the potential to contribute to the climate effects of aerosols (Kerminen et al., 2018). Such particles form a complex external aerosol mixture influenced by local co-pollution, meteorology, and atmospheric processes (Rönkkö and Timonen, 2019). Anthropogenic emissions overall can also affect greatly on the frequency and intensity of NPF events in urban air (Saha et al., 2018). Additionally, emissions of diesel vehicles can include metal-containing particles, which can be found in a separate size mode from non-volatile partiles near 10 nm (Kuuluvainen et al., 2020)~~, and metallic~~. Metallic combustion-originated nanoparticles have also been found to exist in the brains (Maher et al., 2016).

In this study, the EUCAARI inventory has been updated for more realistic, measurement-derived PSDs originating from road transport. PSDs between 1.2 and 800 nm particles measured in a traffic-influenced street canyon in Helsinki, Finland, were incorporated into the inventory in order to better represent real-world particle emissions from vehicles. The updated inventory was then applied in the PMCAMx-UF model, and the effects of updating were studied at different spatial and temporal scales, compared to the observational data, and contrasted with NPF. The simulated period (May 2008) was photochemically relatively active, which elevates NPF to the major source of new particles. This period was chosen because the same period has been simulated in several other related studies as well, providing plenty of comparable data and pre-defined input files for emissions and meteorology. Since the street canyon measurements were performed in 2017—using more recent technologies for PSD measurements—trends of urban aerosol and vehicle emissions were used to scale the determined emissions from 2017 to 2008.

2 Experimental data

The original EUCAARI inventory was updated using PSDs and CO_2 concentrations measured at the Mäkelänkatu supersite, located in a highly trafficked street canyon in Helsinki, Finland. The street canyon measurements were performed in May 2017 and in May 2018. PMCAMx-UF simulations were done for May 2008 as in the previous PMCAMx-UF studies over Europe (Fountoukis et al., 2012; Ahlm et al., 2013; Baranizadeh et al., 2016; Julin et al., 2018). More recent measurements for determining traffic emissions were used because PSD measurements down to ∼1 nm were unavailable in 2008. Hourly PSD data are also available for several atmospheric measurement stations across Europe for May 2008.

2.1 Determining traffic emission factors

The Mäkelänkatu supersite is a continuous measurement site operated by the Helsinki Region Environmental Services Authority (HSY). It is located at a curbside of a highly trafficked (28 000 vehicles per workday) street canyon about 3 km north of the city center of Helsinki, Finland. About one tenth of the traffic is comprised of heavy-duty vehicles. The detailed information on the supersite and the measurements performed in May 2017 can be found elsewhere (Kuuluvainen et al., 2018; Hietikko et al., 2018; Olin et al., 2020). Additionally, the composition of NCA (volatile and non-volatile fractions), measured at the Mäkelänkatu supersite in May 2018 (Lintusaari et al.) and the particle compositions (black carbon (BC), sulfate (SO_4), and primary organic aerosol (POA) fractions) in diluted exhaust of a diesel bus, obtained from a simulation with an aerosol dynamics model coupled with a computational fluid dynamics (CFD) ~~simulation~~ model (Olin, 2013), were used in splitting the EFs further into chemical compound categories specified by the EUCAARI inventory.

PSDs ($\mathrm{d}N/\mathrm{d}\log D_\mathrm{p}$) were determined with the combination of a particle size magnifier (PSM), two condensation particle counters (CPCs), and a differential mobility particle sizer (DMPS), as described by Olin et al. (2020). In addition to the study by Olin et al. (2020) taking only a large-particle dilution ratio (DR$= 8.2$) of the used bridge diluter into account, DR is now afterward corrected for very small particles~~using a DR curve determined~~ . The correction was done using a DR-vs-D_p curve determined in an inverse modelling study with CFD (Olin et al., 2019). The corrected DR for the first two size bins (1.2–3 nm and 3–7 nm) are 10.7 and 8.8, instead of the constant value of 8.2.

The concentrations (N in cm^{-3}) of every size bin of the determined PSDs were converted to EFs (n in $1/\mathrm{kg_{fuel}}$) using simultaneous CO_2 concentration measurements (examples shown in Fig. S1) in 1 min time resolution, as was done for the NCA concentration by Olin et al. (2020). ~~The~~ To express all data in similar time resolution, the PSDs measured with the DMPS in 9 min ~~time~~ resolution were interpolated to 1 min resolution before calculating the EFs. Whereas NCA measured at the curbside probably originates from the studied street or via atmospheric NPF, larger particles—having longer atmospheric lifetime—can be originated also from larger area, including nearby streets or the whole urban area. Nevertheless, due to the fact that linear fitting of the particle concentrations from every size bin against the CO_2 concentration is possible (Fig. S1), their relation to the traffic is evident, although all particle sizes may not be originated from the studied street. The calculated EFs are here represented as an emission factor particle size distribution (EFPSD, $\mathrm{d}n/\mathrm{d}\log D_\mathrm{p}$), presented later in Sec. 3.2.2.

2.2 Atmospheric measurement stations

Simulation results are compared with the observations from several atmospheric measurement stations across Europe. PSD data from six measurement stations from the EUSAAR (European Supersites for Atmospheric Aerosol Research) network and from the SMEAR (Station for Measuring Ecosystem-Atmosphere Relations) III station in Helsinki were utilized in the model evaluation.

The selected EUSAAR stations (Kulmala et al., 2011) represent different types of locations: Aspvreten, Sweden, and Mace Head, Ireland, are located in coastal areas, Hyytiälä, Finland, and Vavihill, Sweden, are located in rural continental areas, Ispra, Italy, and Melpitz, Germany, are not in close vicinity of pollution sources but are still affected by traffic emissions. The

SMEAR III station in Kumpula in Helsinki, Finland, is located in an urban background area and the nearest busy road (50 000 vehicles per day) is separated from it by a 150 m band of deciduous forest (Järvi et al., 2009). The Kumpula station is less than 1 km away from the Mäkelänkatu station; thus, they are quite comparable. However, the Mäkelänkatu station is much more affected by traffic because it is located at a curbside of a busy street canyon (Okuljar et al., 2021). They fall inside the same computational grid cell of the PMCAMx-UF model in this regional scale application.

3 Simulations

Simulations were performed with the PMCAMx-UF model for 1–29 May 2008, similarly to Julin et al. (2018). The results from the first two days were omitted from the analysis to minimize the effects of uncertain initial conditions. The model was run with the original and with the updated emission inventory. The effects of traffic emissions and atmospheric NPF were also examined by performing the model runs also without NPF.

3.1 Model description

The three-dimensional regional chemical transport model PMCAMx-UF simulates both the size-dependent particle number and chemically resolved mass concentrations (Jung et al., 2010). Vertical and horizontal advection and dispersion, wet and dry deposition, and gas-phase chemistry descriptions are based on the publicly available CAMx (Comprehensive Air Quality Model with Extensions) air quality model. Aerosol dynamics processes in PMCAMx-UF, NPF, condensation, and coagulation, are modelled using the DMAN (Dynamic Model for Aerosol Nucleation) by Jung et al. (2006). DMAN tracks the aerosol mass and number distributions using the TOMAS (Two-Moment Aerosol Sectional) algorithm (Adams and Seinfeld, 2002), in which particles are logarithmically divided into 41 size bins between 0.8 nm and 10 μm.

This study used the most recent version of the PMCAMx-UF model, used also by Julin et al. (2018). In this version, particles contain 15 chemical components: POA, BC, SO_4, ammonium (NH_4), five secondary organic aerosol (SOA) components separated according to their volatility, crustal material, nitrate, sodium, chloride, a surrogate amine species, and water (H_2O). The model predicts NPF rate from the sum of the rates of three included NPF mechanisms: the cluster kinetic model ACDC (Atmospheric Cluster Dynamics Code, McGrath et al. (2012); Olenius et al. (2013))-based sulfuric acid (H_2SO_4)–ammonia–H_2O and H_2SO_4–dimethylamine–H_2O mechanisms and the classical nucleation theory-based H_2SO_4–H_2O mechanism (Vehkamäki et al., 2002). The used computational grid covered the European domain with a 36 km $\times$ 36 km horizontal grid resolution and 14 vertical layers reaching an altitude of 6 km. More detailed information of the used model version can be found in Julin et al. (2018).

3.2 Updating the emission inventory

3.2.1 Extracting the road transport-related particle emissions from the EUCAARI inventory

Hourly gridded particle emissions in the EUCAARI emission inventory are separated into 15 source categories and sub-categories. One of the categories is for road transport and it is further separated to four sub-categories: gasoline, diesel, liquefied petroleum gas, and non-exhaust (e.g., from tires or brakes) emissions. ~~Due to the unavailability of the~~ Because the particle number emission rates in 41 size bins in a source category-level were not openly available, updating only road transport-related emissions was not straightforward. The road transport-related emissions were extracted from the inventory—reporting the particle number emissions as a sum of all 15 sources (separated in all size bins and components)—through a Positive Matrix Factorization (PMF) analysis.

The most optimal solution from the PMF analyses was obtained when the inventory was represented with 16 factors, according to the decrease of the normalized error with increasing the number of factors. Due to an inexact nature of PMF, the optimal solution was not obtained with 15 factors even though the inventory has been constructed with 15 sources. Figure ~~S1~~ S2 presents maps of the monthly mean abundances of all 16 PMF factors. The factors 5, 6, 7, 11, and 12 have features reflecting real traffic patterns. However, Fig. ~~S2~~ S3 presenting means of diurnal variations of the abundances of the PMF factors in Kumpula/Mäkelänkatu and Melpitz displays that reasonable diurnal cycles for ~~the~~ both stations are seen only with the factors 6~~and 7. The~~, 7, and 11. Of these, only the PSD from the factor 6 ~~was selected to represent the road transport-related sub-category which is updated in this work, according to its map features~~ (Fig. ~~1a) , diurnal variation (Fig. 1b), and PSD (Fig. 1c). The~~ S4) corresponds to the on-road diesel exhaust PSD, presented by Denier van der Gon et al. (2009), which is also a bimodal distribution having the modes at 23 and 57 nm. The road transport-related source in the original EUCAARI inventory was available as the total particle mass emission rate. Thus, the map and diurnal variation of the particle mass emission rate from the factor 6 ~~in Kumpula/Mäkelänkatu~~ were compared with the ones from the EUCAARI inventory (Fig. ~~1b)agrees well with the diurnal variation of the measured traffic density in Mäkelänkatu, in 2017, presented by Olin et al. (2020). PMF~~ S5). It can be seen that the map features, diurnal variations, and the level of the values overall are very comparable with some exceptions, such as some ship routes in the factor 6~~presumably corresponds to on-road diesel exhaust emissions because the PSD of the factor (Fig. 1c) agrees well with the on-road diesel exhaust PSD presented by Denier van der Gon et al. (2009),~~ due to inexactness of PMF. However, marine areas were omitted from the following emission updates.

Finally, the PMF factor 6 was selected to represent the road transport-related sub-category updated in this work. Although the road transport-related emissions in the inventory consist of four sources, only the ~~diesel-related PMF~~ factor 6, which is presumably only diesel-related, was used in updating the inventory because it was connected to road emission with high certainty. Omitting the other sub-categories (gasoline, liquefied petroleum gas, and non-exhaust emissions) ~~causes that the previously underestimated particle emissions (sub-50 nm) still remain slightly underestimated in this study. Nevertheless, the underestimation~~ is not significant because the abundances of the other factors are lower compared to the factor ~~6. Due to inexactness of PMF, some ship routes are seen in the factor~~ 6 ~~; however, no changes to the emissions for marine areas were made~~and because using this factor already slightly overestimates the mass emissions (Fig. S5).

3.2.2 Emission factor particle size distribution

Figure 1 ~~c~~ presents the EFPSD derived from the PSD measurements in Mäkelänkatu. Its shape agrees well with the shape of the difference PSD (background PSD subtracted from the PSD measured when wind blew from the road) from the same experiment reported by Hietikko et al. (2018), with the exception of a slightly higher soot mode in the difference PSD. The agreement implies that deriving an EFPSD from bin-by-bin calculation of EFs using CO_2 concentrations is an acceptable method. The concentration at the first size bin (1.2–3 nm) is calculated as the average (circled dot) of two values: the value (dot) derived from the experiment in 2017 and the value (circle) derived from the experiment in 2018 (Lintusaari et al.). This was due to a reason that the concentration of the first bin was lower than the next bin (3–7 nm) with the year 2017 data. This is unexpected and possibly caused by uncertainties involved in the detection and penetration efficiency corrections for the particles in the first bin (NCA-sized). The efficiencies of NCA are very low and thus prone to high relative uncertainty. The EF of NCA from the study by Lintusaari et al.—which, in that case, is higher than the EF of the next bin—was utilized because more sophisticated efficiency calculations were performed there and is thus considered more accurate. Particles in the first two size bins simulated with the PMCAMx-UF model (0.8–1.3 nm) originate only from NPF processes; such particles also cannot be measured using aerosol instrumentation.

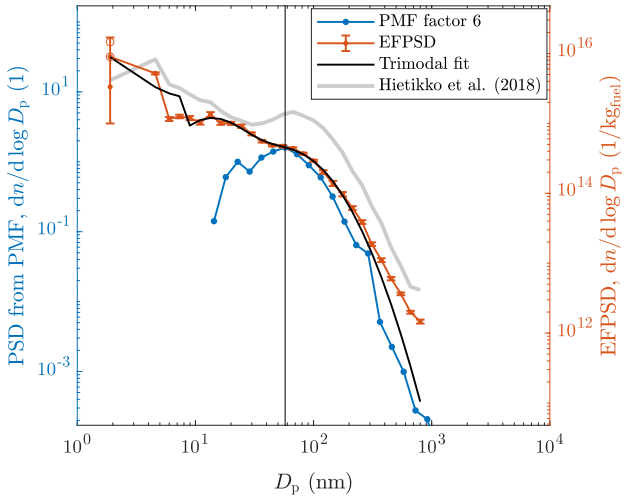

Figure 1. ~~Monthly means of (a) particle number emission rate and (b) its diurnal variation in Kumpula/Mäkelänkatu~~ PSD from ~~the PMF factor 6. (c)~~ PMF factor 6 and ~~measured~~ EFs measured at Mäkelänkatu as PSD (EFPSD) together with the trimodal fit on ~~the EFPSD~~it. The vertical line at 57 nm denotes the highest D_p considered in the updating process and is also the size where the PSDs overlap. The shape of the difference PSD measured at Mäkelänkatu (Hietikko et al., 2018) is also shown for comparison (the data is scaled so that it can be easily compared with the EFPSD data).

The EFPSD, expressed in the unit of $1/\mathrm{kg_{fuel}}$, was converted to correspond to the emission source input of the model, expressed in the unit of $\mathrm{m^{-2}h^{-1}}$ in the following way. The yearly CO_2 emissions from road transport in the EU was $7.9\times$

10^{11} kg in 2008 (European Environment Agency, 2021). It corresponds to the fuel combustion of $2.5 \times 10^{11}\,\mathrm{kg_{fuel}a^{-1}}$, which was further corrected with the factor of the population count within the simulation domain and in the EU, resulting in the fuel combustion of $5.7 \times 10^{7}\,\mathrm{kg_{fuel}h^{-1}}$. The EFPSD, determined for the year 2017, expressed as PM2.5 is $0.31\,\mathrm{g/kg_{fuel}}$. However, due to tightened emission regulations, led to introduction of vehicles emitting fewer soot particles (DieselNet, 2021), e.g., by equipping vehicles with a diesel particulate filter (DPF) (Wihersaari et al., 2020), the EF of PM2.5 has ~~probably~~ been higher in ~~2008.~~ 2008 (EMEP, 2021). Decreasing BC and PM2.5 concentrations in Mäkelänkatu have also been observed from the long-term measurements since 2015 (Barreira et al., 2021; Luoma et al., 2021). The determined EF of PM2.5 was thus estimated to correspond the EF for the year 2008 using the yearly decrease rate of PM2.5, $7.1\,\%\mathrm{a}^{-1}$ (Luoma et al., 2021), resulting in the EF of $0.87\,\mathrm{g/kg_{fuel}}$. That leads to the value of $4.9 \times 10^{7}\,\mathrm{gh^{-1}}$ for the simulation domain. This value is the same for the hourly emission of PM2.5 obtained from the PMF factor 6, which leads to that the levels of EFPSD and the PSD from PMF match with each other ~~. Their concentration~~ at D_p of 57 nm~~also overlap and the~~. The yearly decrease rate of PM2.5 ($7.1\,\%\mathrm{a}^{-1}$) was, however, reported as statistically not a significant trend (Luoma et al., 2021) and also it only covers the trend between years 2015 and 2018. Thus, a trend was also estimated with the data from Kumpula, which fully cover the years between 2008 and 2017. Applying a seasonal Mann-Kendall test and Sen's slope estimator—as done by Luoma et al. (2021)—to the particle number concentration at 56 nm gives the yearly decrease rate of $4.4\,\%\mathrm{a}^{-1}$ for the years between 2008 and 2017. Since this trend is for Kumpula, the trend for Mäkelänkatu could be around $7.1\,\%\mathrm{a}^{-1}$ because the trends of other quantities for Mäkelänkatu were found to be approximately 2-fold than for Kumpula in the study by Luoma et al. (2021). Additionally, the PM2.5 trend was calculated from the data of yearly (1990–2019) road transport emissions (without road, tyre, and brake wear) in Finland, reported by EMEP (2021). The decreasing trend calculated for the years between 2008 and 2017 is $6.0\,\%\mathrm{a}^{-1}$, which corresponds relatively well to the trend applied here ($7.1\,\%\mathrm{a}^{-1}$).

Because fuel efficiency has developed during the years, $\mathrm{CO_2}$ emissions from road transport have been on different levels in 2008 and in 2017. The method of determining EFs using $\mathrm{CO_2}$ concentrations gives the EFPSD with respect to kilograms of fuel combusted. Therefore, it can be applied to any year. However, the total amount of combusted fuel in the computational grid with respect to time has changed, leading to the need of scaling the time-based particle emission rates—which is the form of the emission input of the model—upwards from year 2017 to year 2008. This scaling has, however, already been performed when the EFs were scaled using the trends of PM2.5, because ambient PM2.5 concentrations have decreased not only due to equipping vehicles with a DPF but also due to the fact that the total amount of fuel combusted has decreased.

The shapes of the ~~PSDs~~ PSD from PMF factor 6 and the estimated EFPSD beyond 57 nm agree relatively well, suggesting that the soot mode was estimated quite accurately already in the original EUCAARI inventory. Because the PSDs of the soot modes lie on similar levels, the emitted particle mass was affected only marginally in the update. The ~~concentration of the soot mode particles is also~~ soot mode is assumed to be ~~estimated with an adequate accuracy~~ already estimated well also because exhaust soot measurements have much longer history than measurements of smaller particles~~and because~~. Additionally, the soot particle concentration is not as sensitive to driving and environmental parameters as of smaller particles. 57 nm was selected as the upper limit for which the updating process was applied, i.e., no changes to the original inventory for $D_\mathrm{p} > 57$ nm was made.

3.2.3 Uncertainties involved in updating the emission inventory

Here we elaborate further on the uncertainties involved in representing the road transport-related emissions Europe-wide with a single EFPSD determined from the measurements in Mäkelänkatu in 2017.

Estimating the level of the EFPSD for the year 2008 from the measurements performed in 2017 includes high uncertainty because the used yearly decrease rate of PM2.5 by Luoma et al. (2021) was determined from the measurements beginning not until 2015 and includes its own uncertainty (including statistically not a significant result). Nevertheless, the scaling of the soot modes was a primary objective here because, hence, the update of the inventory considers only updating the shape of the emitted PSD (below 57 nm), but not its level overall. Additionally, estimating the possible change of the shape of the PSD during the years was not possible. It is, nevertheless, expected that while equipping vehicles with DPFs, soot particle concentrations are decreased but also the smaller particles may have been decreased. That is because a DPF can filter small particles also—if they are primarily emitted—and because fuel sulfur content has been reduced (DieselNet, 2021), leading to fewer particles formed via sulfur-driven nucleation (Maricq et al., 2002; Kittelson et al., 2008). It should, however, be noted that while the particle emissions from diesel vehicles have been decreased over the last few years, the gasoline vehicle fleet has begun to emit more particles due to the increased favoring of gasoline direct injection technologies (Awad et al., 2020). On one hand, this increases the uncertainty in estimating the EFPSD for 2008 using the data from 2017; but on the other hand, it provides better estimation on the air quality affected by the modern vehicle fleet.

Vehicle fleets differ among countries, e.g., by fuel selection and by the ages of the vehicles. The average vehicle age in Finland is similar to European average, while diesel vehicles are on average slightly less popular in Finland than in rest of Europe (Eurostat, 2021). It should, however, be noted that averaging of vehicle ages or fuel types over Europe is not the most representative in terms of the average emissions or particle exposure because there are countries having old vehicle fleet with mostly diesel vehicles—a combination with a plenty of soot emissions—but also countries having new vehicle fleet also with mostly diesel vehicles—a combination with the least particle emissions. In addition, there are countries with other possible mixtures of fleet ages and fuel types of vehicles as well.

Particle emissions depend on driving parameters, such as on engine load (Rönkkö et al., 2006). Therefore, particles emitted on an urban street, such as Mäkelänkatu, do not fully represent the particles emitted on other road types, such as on motorways, where higher engine loads are utilized. However, there are signal-controlled intersections on Mäkelänkatu near the measurement site providing also data for emissions with higher engine loads—during accelerations.

Particle emissions depend also on environmental parameters, such as temperature (Mathis et al., 2004; Olin et al., 2019) and radiation (Olin et al., 2020). Therefore, particle emissions can differ between nighttime and daytime. Here, we aim for a first level approximation of PSDs of the emissions using a single EFPSD—for the the most representative average covering the whole vehicle fleet, driving parameters, and environmental parameters in May. Despite this simplification, it is a useful first step in determining the importance of these particles. To our knowledge, in addition to the Mäkelänkatu site, no other location with simultaneous CO_2 and PSD measurements down to $\sim$1 nm is available.

Number-based EFs of especially sub-30 nm particles could be quite different if the emissions were determined from measurements performed at a different location, on a different road-type, and at a different time. In contrast, EFs of particles larger than 30 nm—mainly soot—would possibly differ much less with differing location or time. Nevertheless, the approach in this study still represents the most realistic approximation currently available and it improves the representation of the road traffic-emissions in the original inventory, which excluded all sub-10 nm particles. Emissions of sub-10 nm particles have been applied also in the study by Paasonen et al. (2016), who included a size bin for 3–10 nm particles, based on the TRANSPHORM database (Vouitsis et al., 2013). However, they did not include any modes smaller than 10 nm; thus, this size bin was only an extension from PSDs with larger modes. Kontkanen et al. (2020) compared annual size-binned particle emissions between their estimations from ambient data measured in urban Beijing and the model by Paasonen et al. (2016). They observed that the ambient data suggest significantly more particles in sub-60 nm size range. This is due to the fact that the ambient data represent emissions from a more localized—traffic-influenced—area but also because the smallest particles are omitted from the traffic emissions in the TRANSPHORM database.

3.2.4 Parameters of the emission factor particle size distribution utilized in updating the emission inventory

To utilize the determined EFPSD within PMCAMx-UF, it was transformed to the model size bins through a continuous fit (Fig. 1~~c~~). A trimodal fit consisting of a power law distribution and two log-normal distributions (see the Supplement for the detailed equation) is used because there seems to be features of two log-normal distributions—as typical in vehicle exhaust—but the smallest particles cannot be fitted very well to any log-normal distribution. A power law distribution fits moderately and is suggested by theory of simultaneous nucleation and growth processes (Olin et al., 2016). The parameters of the fit are presented in Table 1. It is interesting that trimodal size distributions of non-volatile particles—with quite similar particle sizes to the ones found in this study—were also detected in diesel exhaust by Kuuluvainen et al. (2020)~~, who~~. They conclude that the mode in the middle is originated from lubricating oil, whereas it is here associated with nucleation-originated particles.

The contribution of the road transport-related particle number emissions (from the PMF factor 6, which is presumably related only to diesel vehicles) to the total emissions from ~~the~~ all emission sources was averagely 8 % in the original inventory. In updating the inventory, ~~the~~ these road transport-related particle number emissions were increased to a 26-fold level, resulting in the increase of the total number emissions to a 3-fold level. Hence, in the updated inventory, the contribution of ~~the~~ these road transport-related particle number emissions (from diesel vehicles) to the total emissions becomes 69 %. Due to the lack of all sub-10 nm particle emissions in the original EUCAARI inventory, sub-10 nm particle emissions in the updated one come exclusively from road transport. By considering only the number concentrations of ultrafine particles (UFP, sub-100 nm particles), the road transport-related emissions were increased to a 28-fold level. This resulted in that the total UFP number emissions were increased by a factor of 3.1.

Vehicle-emitted particles originate primarily via three routes: in-cylinder processes (soot mode, ash particles, non-volatile core), nucleation after the exhaust pipe (nucleation mode), and a less-known source of NCA (power law mode). Therefore, a trimodal fit suits well in separating particle composition between the three sources. However, it should be noted that the vehicle exhaust particle formation is a complex process and this approach is only an approximate~~; e. g.,~~. Studies such as

Table 1. Mode parameters of the trimodal fit on the measured EFPSD and the estimated particle composition.

Mode name	Power law	Nucleation	Soot
n (10^{14}/$\mathrm{kg_{fuel}}$)	115	17.2	6.44
$\mathrm{D_1}$ (nm)[a]	1.2	–	–
$\mathrm{D_2}$ (nm)[b]	8.0	–	–
α[c]	-1.2	–	–
CMD (nm)[d]	–	13.4	59.0
GSD[e]	–	1.8	1.9
BC mass fraction	0.158	0	0.688
$\mathrm{SO_4}$ mass fraction	0.128	0.152	0.064
POA mass fraction	0.714	0.848	0.248

a,*b* Diameters of the smallest and largest particles of the mode
c Slope parameter
d Count median diameter
e Geometric standard deviation

Kuuluvainen et al. (2020) and Alanen et al. (2020) divide the non-volatile PSDs of internal combustion engine emissions into three categories, based on PSDs and particle morphology studies, and nucleation mode observed in vehicle exhaust does not always require $\mathrm{H_2SO_4}$-driven formation process.

To add particles to the original road transport-related PSD, a selection for their chemical composition was needed. Because measuring chemical composition for sub-50 nm particles is challenging, this study relies on CFD-simulations of particle composition 10 m behind a diesel-fueled bus by Olin (2013). They consist of a situation where a Euro III bus is driving at a speed of 40 km/h with the engine power of 40 % of the maximum (see the Supplement for a more detailed description). The CFD-simulations give mass fractions of BC, $\mathrm{SO_4}$, POA, and $\mathrm{H_2O}$ for the nucleation and soot modes. The road transport emissions in the original EUCAARI inventory consist solely of BC, $\mathrm{SO_4}$, POA, and crustal material~~; thus~~. Thus, the CFD-simulated mass fractions can be directly utilized in the inventory, with the exception of $\mathrm{H_2O}$ which is not included in the emissions due to an equilibrium-type behavior of $\mathrm{H_2O}$ dynamics in the model. The chemical composition for the power law mode is determined by, firstly, assuming a fraction of 16 % of non-volatile particles (the non-volatile fraction of NCA (Lintusaari et al.)) and, secondly, assuming the nucleation mode composition for the remaining volatile part. The non-volatile part is ~~assumed to be~~ here lumped together with BC due to the lack of more specific information on its composition and because adding an extra component would have required several modifications to the model code. BC together with the unknown non-volatile part is abbreviated here to BC*. Figure 2 presents the particle chemical composition of the traffic-emitted particles as a function of D_p in the original and in the updated inventory. The composition between 10 and 57 nm is modified to contain more POA and less BC because nucleation mode particles—consisting mainly of POA—were considerably added. Nucleation mode-sized particles were also in relatively low $\mathrm{SO_4}$ concentration in the original inventory, but more $\mathrm{SO_4}$ is included in

the updated inventory. No particles below 10 nm were included in the original inventory. Importantly, the inventory does not include metallic ash particles, that have been reported to contribute particle emissions especially in ultrafine particle size range.

The selection of the CFD-simulations of a diesel-fueled bus for determining chemical composition of particles was further elaborated by examining other related studies as well. Kostenidou et al. (2021) measured chemical composition of particles emitted by different gasoline- and diesel-fueled Euro 5 light-duty vehicles over different transient driving cycles on a dynamometer. Calculated from the reported EFs, the mass fractions of BC, SO_4, and POA in the total aerosol were 0.58–0.98, 0.00–0.30, and 0.02–0.15, respectively. Similarly, Pirjola et al. (2019) measured a diesel-fueled Euro 4 light-duty vehicle and reported the BC, SO_4, and POA mass fractions of 0.81–0.88, 0.00–0.03, and 0.11–0.18, respectively. These mentioned mass fractions are comparable to the mass fractions in the soot mode from the CFD-simulations (Table 1). However, it should be noted that in the mentioned studies, SO_4, and POA were measured using aerosol mass spectrometers, which do not efficiently detect particles smaller than ~ 50 nm. Therefore, the composition of the nucleation mode, or especially of the power law mode, is barely covered in the measured compositions and studies related to these compositions are very scarce. According to the formation principle of nucleation mode particles, they do not contain BC; thus, POA dominates in the mass fractions of the nucleation mode (Table 1) as it dominates in the mass fractions of the volatile (SO_4 and POA) part of the soot mode. Hao et al. (2019) collected PM2.5 particle samples on filters from a highway tunnel in China and reported the BC, SO_4, and POA mass fractions of 0.12, 0.09, and 0.34, respectively. These values lie in the range between the mass fractions of the nucleation and soot modes from the CFD-simulations. In conclusion, due to the scarcity of studies on chemical composition of vehicle-emitted particles and because the CFD-simulated mass fractions (of a diesel bus only) are reasonable according to the other studies (including tailpipe emissions of both gasoline- and diesel-fueled light-duty vehicles and emissions from a real traffic mixture from a road tunnel), the CFD-simulated ones were used here to cover the whole vehicle fleet. In addition, this study primarily focuses on the updating of the shape of the PSD, but not on the exact chemical composition of emitted particles, which was, however, required to be estimated for running the model with the updated inventory.

3.3 Simulation results

3.3.1 Comparing simulated particle number concentrations with observations

Particle number concentrations from the PMCAMx-UF simulations were first compared to the ones observed at the measurement stations. Figure 3 presents hourly means of number concentrations of particles smaller than 10 nm ($N_{<10}$) and larger than 10 nm ($N_{>10}$) with the original (orig) and updated (upd) emission inventories. The data of $N_{<10}$ are shown only for the stations that had reliable PSD measurements in sub-10 nm size range. The lower D_p-limit in $N_{<10}$ and the upper D_p-limit in $N_{>10}$ for the simulated and the observed values depend on the corresponding limits of the PSD measurements and vary slightly between the stations. There are overestimations in simulated concentrations of particles between 10 and 50 nm and slight underestimations for particles larger than 100 nm ($N_{>100}$) in the previous studies (Baranizadeh et al., 2016; Julin et al., 2018) with the PMCAMx-UF model, possibly due to missing condensable vapors and particle growth mechanisms (Baranizadeh et al., 2016). Even higher overestimations but also underestimations are seen in $N_{<10}$ (Fig. 3a); however, the most notable underestimations

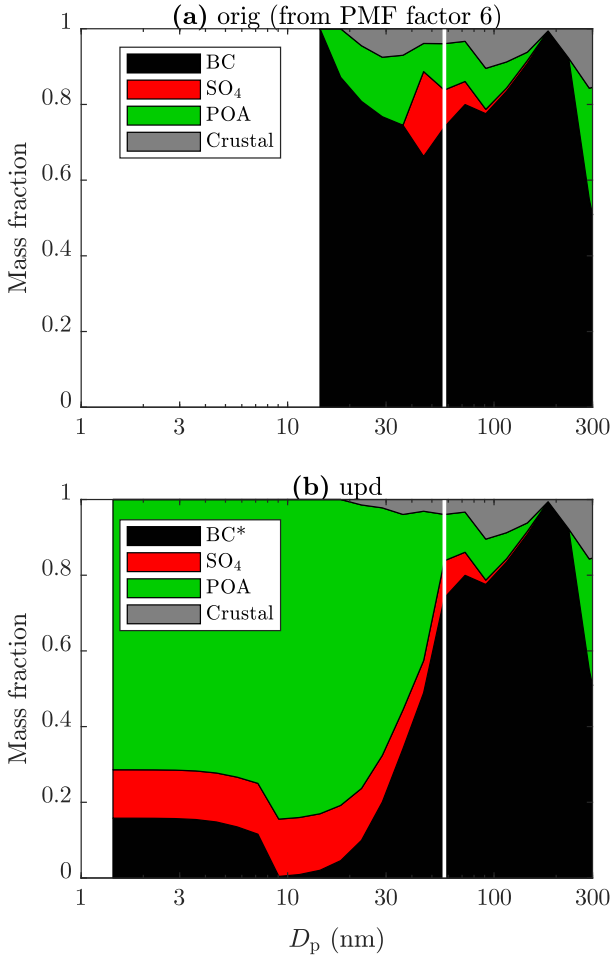

Figure 2. Particle chemical composition (**a**) of the PMF factor 6 and (**b**) after updating the emission inventory. The composition of the emitted particles larger than 57 nm (vertical lines) remains unchanged and larger than 300 nm are not shown due to their irrelevance.

are now overcome when using the updated emission inventory (Fig. 3c). The highest overestimations in $N_{<10}$ still exist, especially for rural locations. In the case of $N_{>10}$, no notable differences can be seen between the original (Fig. 3b) and updated emission inventories (Fig. 3d), except slightly increased—but still underestimated—concentrations in the lowest end of the simulated concentrations.

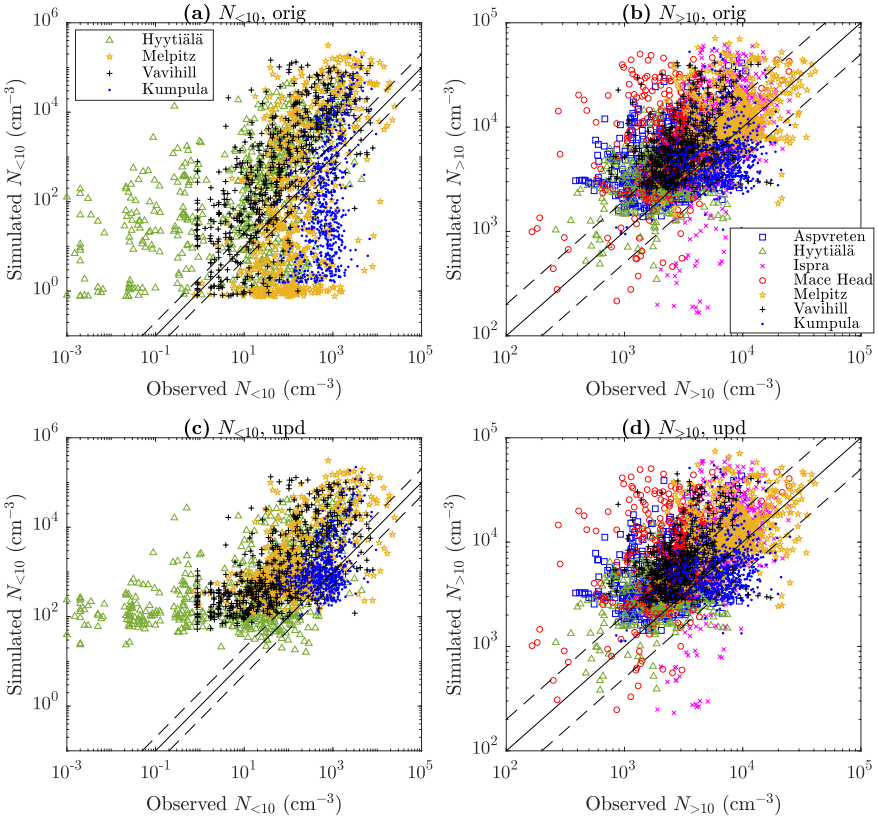

Figure 3. Simulated versus observed number concentrations of particles (**a**, **c**) smaller than 10 nm ($N_{<10}$) and (**b**, **d**) larger than 10 nm ($N_{>10}$) at selected measurement stations with (**a**, **b**) the original and (**c**, **d**) updated emission inventory. All data correspond to hourly means for May 2008. The solid diagonal lines represent 1:1 lines and the dashed ones 1:2 and 2:1 lines. See Fig. S6 for a clearer presentation of the data from the stations with the highest traffic influences only (Melpitz and Kumpula).

355 The agreement and the correlation with the hourly observations and the scatter for $N_{<10}$, $N_{>10}$, and $N_{>100}$ are also presented in Table 2 in terms of normalized mean bias (NMB), correlation coefficient (R), and normalized mean error (NME), respectively. Whereas the values remain nearly constants for $N_{>100}$ after updating the inventory, NMB values for $N_{>10}$ are further increased. The most significant differences after updating the inventory are observed with the logarithms of $N_{<10}$, for which NMB is increased from $+12\,\%$ to $+53\,\%$. Overestimations of the concentrations of the smallest, roughly sub-50 nm,
360 particles—becoming even more substantial after updating the inventory—highlight the possibility of overestimated NPF rates.

On the other hand, overestimation of the simulated $N_{<10}$ can also be perceived as underestimation of the observed $N_{<10}$ due to the inaccuracy (typically underestimating (Kangasluoma et al., 2020)) of PSD measurements in the sub-10 nm size range. It should be noted that there are observations (particularly from Hyytiälä and Vavihill) of very low hourly averages of $N_{<10}$ (below $1\,\mathrm{cm}^{-3}$), which may not be of very reliable data due to low counting statistics and which have thus a major role on the disagreement. In contrast to the agreement, improvements for $N_{<10}$ (logarithms) after updating the inventory can be seen in the correlation and in the scatter: R increases from $+0.37$ to $+0.54$ and NME decreases from $64\,\%$ to $58\,\%$, also seen in Fig. 3a,c as overcoming of the most notable underestimations with the updated inventory. In the case of urban locations, even better improvements are seen, e.g., NME decreasing from $42\,\%$ to $16\,\%$ for Kumpula.

Table 2. Normalized mean bias (NMB), correlation coefficient (R), and normalized mean error (NME) of the simulated particle number concentrations compared to the observed ones. The values in parentheses denote the values with the original emission inventory. The top values are calculated from the ordinary concentrations and the bottom values from the logarithms of the concentrations. The bold values highlight the most notable differences between the inventories (the ~~more intended one being~~ best performing in bold).

	$N_{<10}$	$N_{>10}$	$N_{>100}$
NMB (%)	+1102 (+1066)	+70 (+63)	-12 (-12)
R	+0.30 (+0.30)	+0.40 (+0.38)	+0.61 (+0.62)
NME (%)	1142 (1139)	96 (94)	49 (49)
NMB (%)	+53 (**+12**)	+5.7 (+5.0)	-4.2 (-4.2)
R	**+0.54** (+0.37)	+0.50 (+0.47)	+0.65 (+0.66)
NME (%)	**58** (64)	8.6 (8.5)	10 (10)

3.3.2 Effect of updating emission inventory on relative particle concentrations

Figure 4 presents how much the concentrations of 1.3–3 nm (N_{NCA}), 7–20 nm (N_{7-20}), and all particles (N_{tot}) change after updating the inventory. The concentrations remain nearly unchanged, especially N_{tot}, but are also stretched out to both directions, toward decreased and toward increased concentrations. However, all the histograms are slightly displaced from ~~unity~~ the ratio of one so that increased concentrations are more common. There are also notable extremes in the concentration ratios, especially for NCA (min: 0.0003, max: 4225) denoting that N_{NCA} was decreased or increased with factors of up to several thousands in certain locations on certain days. Although updating the inventory increases emissions for all particle sizes, it also leads to decreased concentrations at certain times in certain areas having a high NPF rate. This results via increased primary emissions of particles increasing the condensation ~~sink~~and coagulation sinks, which can reduce nucleating gaseous precursors and newly formed particles, respectively, and thus lead to ~~lowered NPF rates~~less small particles. Due to a complex relationship between the ~~increase of the condensation sink and the decrease of the NPF rate~~increases of the sinks and the appearance of small particles, updating the emission inventory can change the particle concentrations in both directions. It is clear that

decreased concentrations are related to the connection between NPF and emissions because simulating with NPF processes switched off results in the situation in which updating the inventory only increases the concentrations.

Figure 5 presents the ratios of the concentration change as maps. In contrast to the histograms in Fig. 4, the ratios in the maps are calculated from the monthly mean values, representing the total aerosol exposure of people living in certain areas. The roughest extremes of the ratios do not exist when examining monthly means but there are still sporadic areas in which concentrations were decreased or increased by a factor of ~ 2 (not shown in the maps). The monthly mean concentrations, especially of N_{7-20}, were increased by tens of percents in densely populated areas, especially in Western Europe, but there are also areas having ratios much below or above ~~unity~~ one over marine areas, such as over the Mediterranean Sea.

The ratios of the concentration change calculated from the monthly means are also presented as mean and median values in Table S1. The values for $N_{<10}$ ~~and~~ , $N_{<23}$ (totally unregulated vehicle-emitted particles, $D_\mathrm{p} < 23\,\mathrm{nm}$), and $N_{<100}$ (UFP, $D_\mathrm{p} < 100\,\mathrm{nm}$) are also shown. Additionally, the values are presented as population density-weighted values using the gridded population count data for 2010 from CIESIN (2018). Updating the emission inventory increased total particle count in Europe for the whole month with only $1\,\%$. However, the increase is $2\,\%$ with using the population density-weighting~~, which~~ . That can be interpreted so that the total human exposure on particle number is estimated $2\,\%$ higher when using the updated inventory compared to the original one. Moreover, the increase is $11\,\%$ if only NCA-sized particles are considered. The highest differences are observed with considering particles between 7 and 20 nm, for which the population density-weighting gives the mean increase of $10\,\%$ and the median increase of $4\,\%$. The latter value can be interpreted so that ~~the~~ half of the people within this European domain are, on average, exposed to N_{7-20} with at least $4\,\%$ more than what would have been estimated using the original inventory.

3.3.3 Comparing simulated particle size distributions with observations

The results so far have displayed that the particle concentrations were slightly increased after updating the inventory when the concentrations are averaged over long times and wide areas. The effect of updating the inventory is next examined locally and more temporally, first, by comparing PSDs simulated with the original and with the updated inventory together with the observations. Figure 6 presents monthly means of PSDs at selected measurement stations, separately for mornings (05:00–09:00) and daytime (10:00–14:00). Daytime typically experiences the highest NPF rates, due to the solar radiation cycle, but also high traffic densities. Mornings, instead, have typically even more traffic but not yet solar radiation-ignited NPF. PSDs in the daytime do not differ notably between the original and the updated inventories, with the exception of slightly higher concentrations with the updated inventory in Melpitz and Kumpula for ~5–30 nm particles. Agreement of the daytime PSDs with the observations is fairly good for particles larger than 10 nm, but the overestimation of the simulated particles (or underestimation of the measured particles) smaller than 10 nm can be seen. Melpitz and Kumpula are again different, having higher observed concentrations than the simulated ones. These are locations affected by road traffic, especially Kumpula, and the results hence indicate that traffic emissions may still be underestimated even with the updated inventory. However, it should be noted that the grid cell including the Kumpula station consists of not only urban areas but rural and marine areas too~~;~~ ~~therefore~~. Therefore, the average concentrations within the grid cell are, indeed, expected to be lower than the concentrations

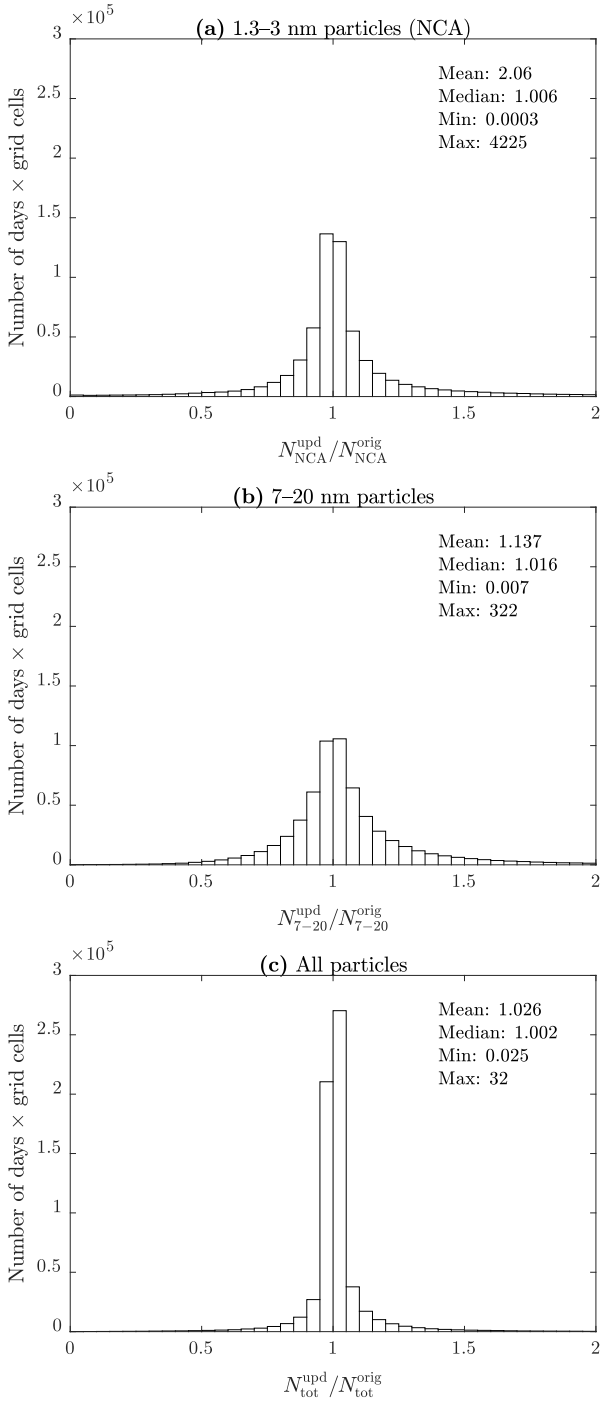

Figure 4. Histograms for grid cell-separated ratios of daily means of (**a**) the NCA concentration (N_{NCA}), (**b**) the concentration of 7–20 nm particles (N_{7-20}), and (**c**) the total particle concentration (N_{tot}) simulated with the updated and with the original emission inventory. Statistics are also presented numerically on the graphs.

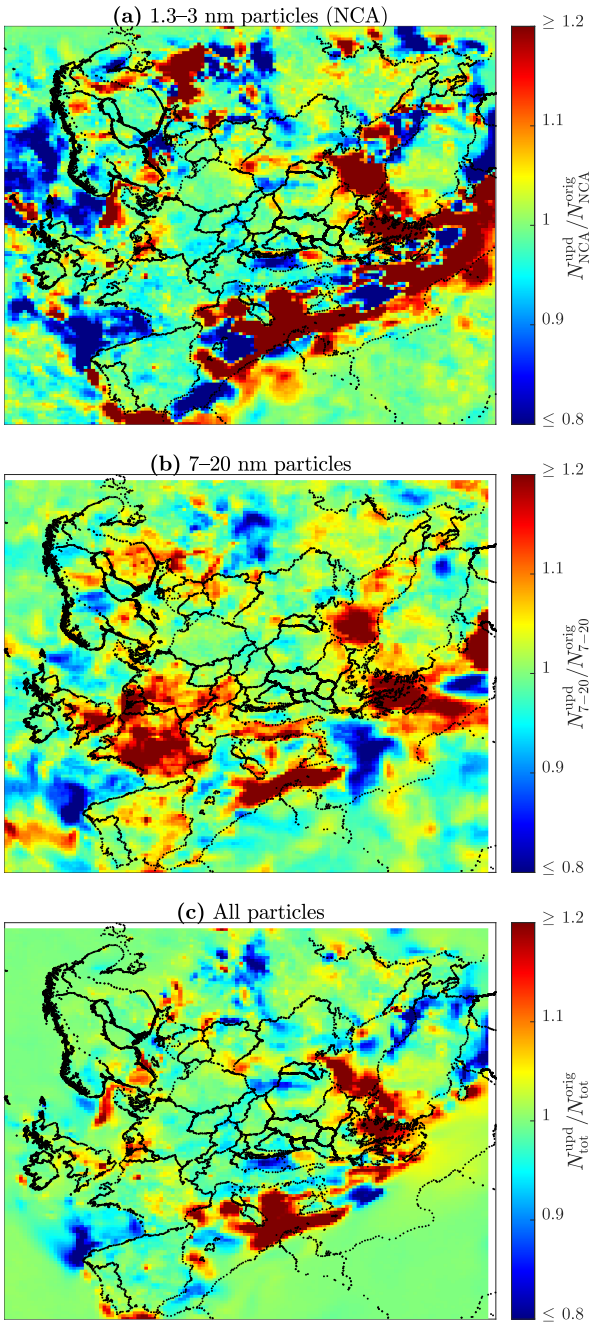

Figure 5. Ratios of monthly means of (**a**) the NCA concentration (N_{NCA}), (**b**) the concentration of 7–20 nm particles (N_{7-20}), and (**c**) the total particle concentration (N_{tot}) simulated with the updated and with the original emission inventory.

within urban areas only. Additionally, there are a busy airport and harbor areas within a radius of 15 km from the Kumpula station. It is certainly possible that, in addition to road transport, other activities, such as aviation and shipping, can also involve underestimated particle emissions. Hence, other anthropogenic particle emission sources may also need to be addressed better in emission inventories, in order to have the simulated PSDs to agree with the measured ones.

In the case of the morning PSDs, differences between the emission inventories are more notable~~; the~~ . The updated inventory predicts levels of sub-30 nm particles up to 3 orders of magnitude higher in areas affected by road traffic (Ispra, Melpitz, and Kumpula) than the original inventory. The use of the original inventory fails to predict PSDs for sub-30 nm particles for the mornings~~but the updated inventory~~. The updated inventory, instead, gives fairly good agreements for the PSDs when the possible underestimation of PSD measurements for sub-10 nm particles are taken into consideration. People exposed to outdoor air in the mornings in urban areas are exposed to sub-30 nm particles remarkably more than would have been predicted using the original inventory. Furthermore, the differences could be even higher within the urban centers, but the used coarse grid resolution cannot capture the effect in more localized scales.

3.3.4 Change of particle composition after updating the emission inventory

Sub-30 nm particles may carry potential health issues because they lie ~~on~~ in the range of the highest lung deposition efficiencies ($> 30\,\%$ for 6–50 nm particles (ICRP, 1994)) and can ~~travel to~~ thus end up in human body, even to the brain via olfactory nerve (Maher et al., 2016). Therefore, they are of high importance, especially in urban areas and if their origin is traffic because emissions from fossil fuel combustion include harmful substances. Simulated particle composition is examined in Fig. 7, as instantaneous composition in Melpitz at 24 May 2008, 09:00–10:00. The selection of this location and time is made to demonstrate how particle composition changes due to updating the inventory while PSD and particle concentration do not significantly change ($N_{\mathrm{tot}}^{\mathrm{upd}}/N_{\mathrm{tot}}^{\mathrm{orig}} = 0.93$, $N_{<10}^{\mathrm{upd}}/N_{<10}^{\mathrm{orig}} = 0.71$). The reason for particle concentrations to even decrease after updating is ~~the lowered NPF rates due to increased condensation sink~~increased condensation and coagulation sinks, as discussed before. In this case, the total NPF rate was lowered to a level of one third of the rate simulated using the original inventory. However, the sinks are actually $\sim 4\,\%$ lower with the updated inventory during the time range presented in Fig. 7. Instead, the sinks just before the time range were $\sim 6\,\%$ higher and even $\sim 10\,\%$ higher in an adjacent grid cell. The effect of increased sinks with the updated inventory on the appearance of small particles is not always observed within a single time step or grid cell but within later time steps or nearby grid cells instead, due to a history effect and transportation of components between the grid cells.

The composition of sub-30 nm particles was changed so that particularly the mass fractions of POA (and slightly BC/BC*) were increased at the expense of the other components, while the composition of particles larger than 30 nm did not substantially change (Fig. 7a,b). The reason why particularly POA and BC/BC* were increased is because ~~they~~ POA and BC* were selected (Sec. 3.2.4) as the main components of the particle emissions of road traffic through CFD-simulations, instead of direct particle composition measurements. Therefore, ~~BC~~ BC* can also comprise of other non-volatile components, such as of metals, in this context. By examining the change of PSD in Fig. 7c, the effect of updating the inventory seems only minor. Nevertheless, by examining the mass size distributions of certain components in Fig. 7d, it can be seen that POA and

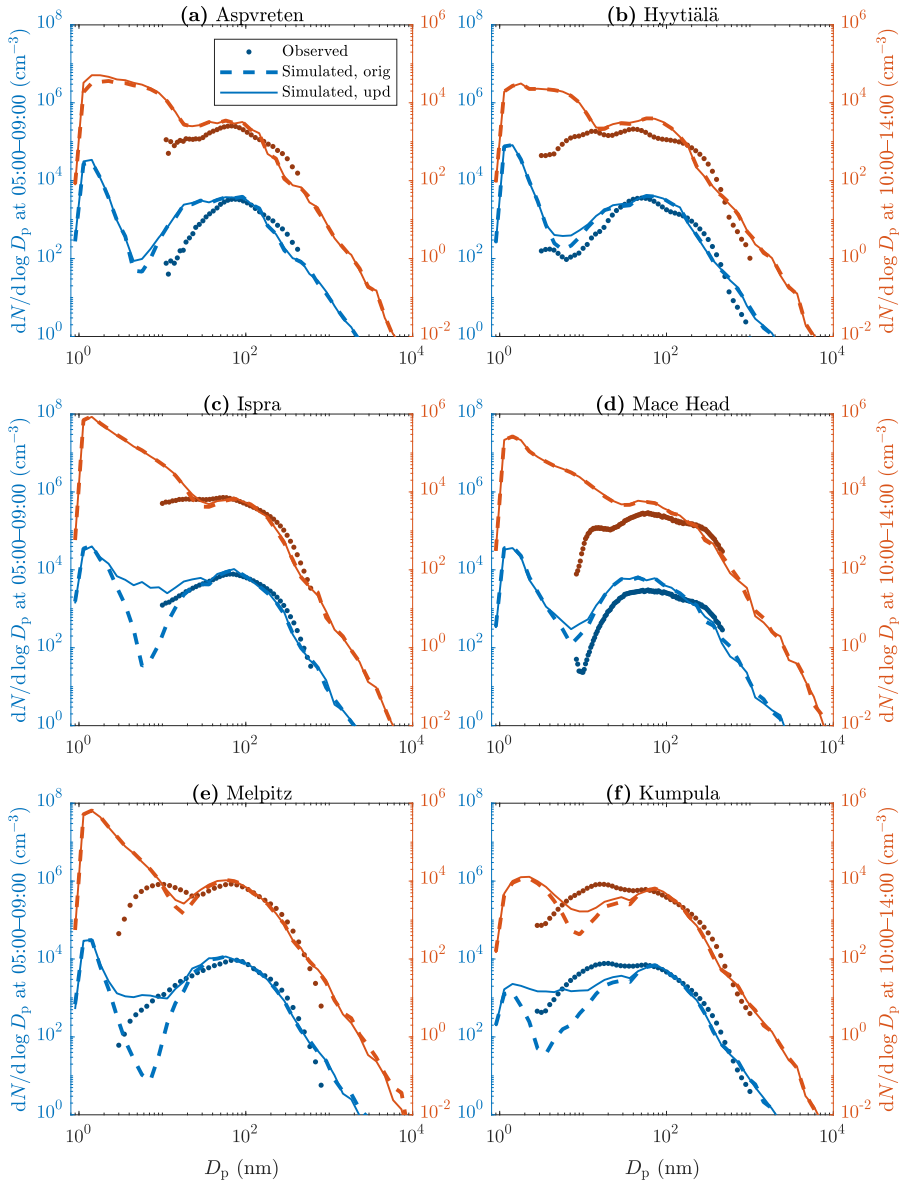

Figure 6. Monthly means of PSDs at selected measurement stations (**a**–**f**) from observations (markers) and from simulations using the original (dashed lines) and the updated (solid lines) emission inventory in the mornings (blue) and in the daytime (red). All times represent local times. Note different axis limits for morning and daytime data.

BC/BC* masses for sub-10 nm particles were increased significantly from nearly zero-levels even though $N_{<10}$ was decreased. In conclusion, whereas the effect of updating the inventory on PSDs is minor in some locations, masses of potentially harmful components in small—efficiently lung-depositing—particles can still be substantially increased and potentially posing elevated health risks.

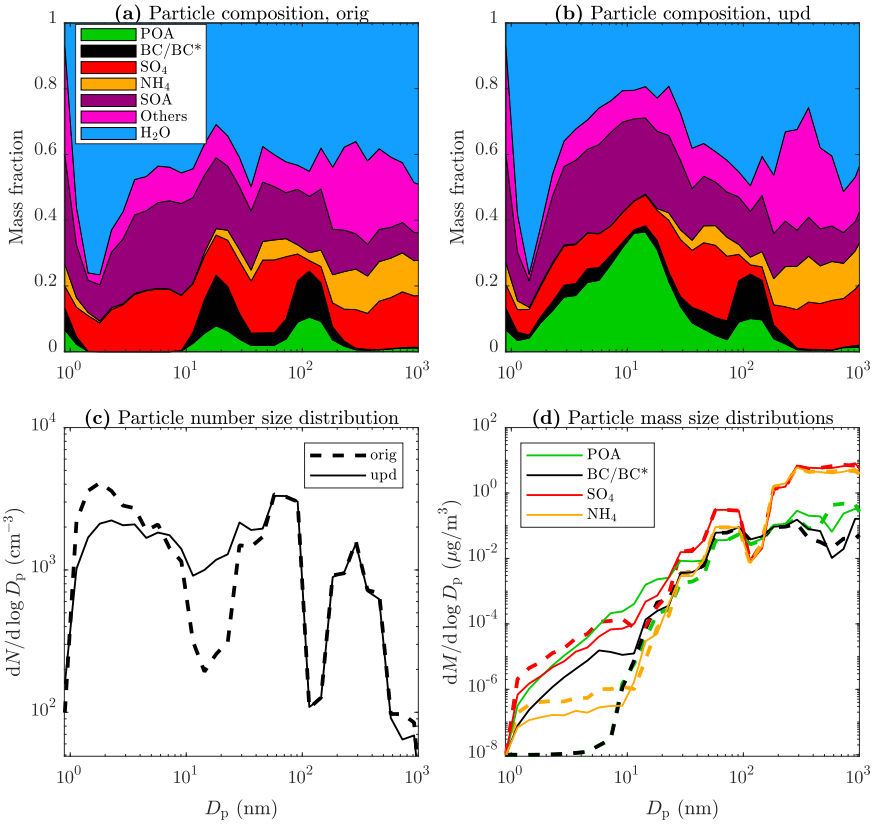

Figure 7. Simulated particle composition in Melpitz, at 24 May 2008, 09:00-10:00 local time, using (**a**) the original and (**b**) the updated emission inventory and simulated particle (**c**) number and (**d**) mass size distributions using the original and the updated emission inventory. Others denote the sum of the remaining components, i.e., crustal material, nitrate, sodium, chloride, and the surrogate amine species.

3.3.5 Comparing the effects of emissions and atmospheric new particle formation on particle size distributions

The effects of primary emissions of particles and atmospheric NPF are examined in Fig. 8, presenting the monthly means of PSDs in ~~London, UK,~~ Melpitz in the mornings and in Hyytiälä in the daytime. In the mornings in ~~London~~Melpitz, NPF plays a minor role only on PSDs if the updated inventory is used~~, which~~ . It is unambiguous due to the location and time range having high traffic densities but not much atmospheric NPF yet. The original inventory, instead, predicts up to 3 orders of magnitude less ~~1.3–30~~ 2–20 nm particles. In the case of Hyytiälä, the effects are opposite instead. Even the updated inventory does not

sufficiently predict the observed aerosol levels (about an order of magnitude lower) when the NPF processes were switched off. Conversely, also the original inventory is sufficient to predict the observed levels and no notable differences are seen between the inventories when the NPF processes were kept on. This was expected, as Hyytiälä is a rural location not greatly affected by road traffic and the daytime is typically associated with atmospheric NPF.

Examining the effects of NPF and emissions within the full European domain displays that the major source of the total particle number is NPF: monthly means of N_{tot} were, in average, decreased with 91 % when the NPF processes were switched off. Without NPF processes, average particle number concentrations increased by 38 % after ~~the~~ updating of the inventory although the total particle number emissions increased to a 3-fold level, due to non-linearities in the model, e.g., coagulation. With the NPF processes, the average particle number increase was only 1 %, which is ~~three times less than~~ one third of what is expected from the increase of the emissions if adding particles would not have a lowering effect on NPF rates.

4 Summary and conclusions

Road transport-related particle number emission factors were determined from measurements performed at the curbside of an urban street canyon in Helsinki, Finland. The emission factors were determined separately for every measured particle size bin (1.2–800 nm) and were presented as an emission factor particle size distribution (EFPSD). Deriving an EFPSD from bin-by-bin calculation of emission factors was found an acceptable method based on the agreement with the reported difference between the PSDs measured with wind blowing from the road and from the background direction.

A separate nucleation mode ($\mathrm{CMD} = 13\,\mathrm{nm}$) and soot mode ($\mathrm{CMD} = 59\,\mathrm{nm}$) are seen in the derived EFPSD but also a considerable number of particles exists in sub-10 nm size range. Notably fewer sub-50 nm particles and no sub-10 nm particles are included in a road transport-related PSD of the EUCAARI emission inventory~~—~~, used in several previous studies~~—~~. This is due to challenges involved in determining emission factors reliably for nucleation mode or smaller particles. In this study, the road transport-related particle emissions of the original EUCAARI inventory were updated using the EFPSD derived here, assuming that it represents the average PSD of the particle emissions from the whole vehicle fleet in Europe.

The PMCAMx-UF model was utilized in simulating aerosol levels for May 2008 over the European domain. The simulations were performed using both the original and the updated emission inventory in order to discover the effect of including the previously ~~underestimated~~ partly excluded emissions of sub-50 nm particles. The model overestimates the concentrations of sub-50 nm particles, regardless of the used inventory. Especially sub-10 nm particles are overestimated ~~with the model~~ and the overestimation became even higher when using the updated inventory. The reason for the overestimations may be related to overestimated new particle formation (NPF) or underestimated particle growth but also to possibly underestimated particle concentrations from the PSD measurements, which are known to become inaccurate for particle sizes below ~10 nm. At least, the overestimations of sub-10 nm particles using the updated inventory are not caused by overestimating their emissions because the overestimations were observed also using the original inventory, in which all sub-10 nm particle emissions were excluded. Nevertheless, the greatest underestimations of the model for sub-10 nm particles were overcome and the correlation between the simulated and the observed concentrations was increased, when the updated emission inventory was used.

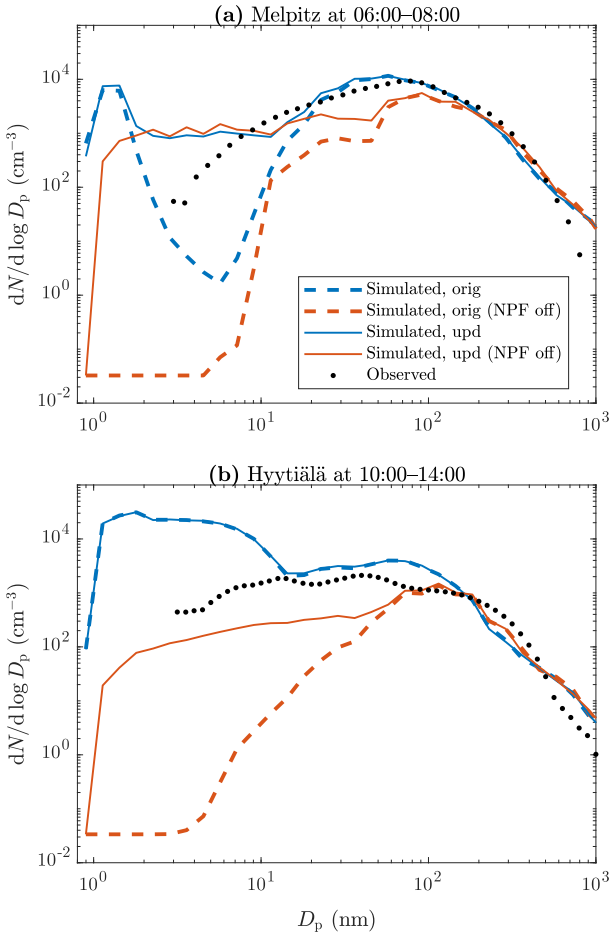

Figure 8. Monthly means of PSDs (**a**) in ~~London~~ Melpitz at 06:00–08:00 local time and (**b**) in Hyytiälä at 10:00–14:00 local time, according to the simulations using the original and the updated emission inventory, both with the NPF processes kept on and switched off. The observed ~~distribution is~~ distributions are also shown~~in **b**~~.

~~There are locations and times having the~~ Ratios of simulated particle concentrations after and before updating the inventory were examined from daily and monthly means of local concentrations. The ratios over and below ~~unity~~ one were observed while the mean and median values were slightly over ~~unity. This denotes that~~ one: the predicted concentrations were increased or decreased with a factor of up to several thousands, depending on the examined particle size range, in certain locations and at certain times after updating the inventory. Although particle emissions were only increased in updating the inventory, it resulted also in decreased concentrations due to increased condensation and coagulation sinks leading to ~~lowered NPF rates~~less small particles. Examining the ratios from the monthly mean concentrations revealed that, although the total anthropogenic particle number emissions were increased to a 3-fold level, the total particle count in Europe for the whole month was increased by only $1\,\%$ and the total human exposure on particle number with $2\,\%$. The highest mean ratios were observed with considering only 1.3–3 nm particles ($11\,\%$ increase) and the highest human exposures with considering only 7–20 nm particles ($10\,\%$ mean increase and $4\,\%$ median increase). The highest increases were observed in densely populated areas, especially in Western Europe.

The updated inventory predicts up to 3 orders of magnitude higher sub-30 nm particle concentrations during the mornings than the original one in traffic-influenced locations. In those urban locations, simulated PSDs also agree notably better with the observed PSDs.

Because sub-30 nm particles deposit efficiently on the human respiratory system, they pose a significant health risk, especially if their origin is ~~fuel-combusting vehicles~~ combustion processes emitting harmful substances. Even in cases in which the simulated particle number concentrations did not change markedly, particulate mass of potentially harmful components can increase substantially in the sub-10 nm size range~~, resulting~~ . This results from the substitution of NPF with traffic as the main origin of those particles.

In conclusion, it is important to consider the emissions of sub-50 nm particles from traffic in more detail in chemical transport models, because the previous underestimations (with the original EUCAARI inventory) of particles are located mainly in populated areas and are the greatest for the most efficiently lung-depositing particle sizes~~, and~~ . Additionally, the underestimations are especially for particle components having possibly harmful effects on human health. Further investigations on traffic-emitted particles are needed in more local scales than with the coarse grid resolution used in this study. The used model can be operated with a grid resolution of down to, e.g., $1\,\mathrm{km}^2$, ~~whenever~~ provided that an emission inventory for that resolution is available. In addition to road transport, other anthropogenic emission sources, such as aviation and shipping activities, may need to be addressed better in emission inventories, because they may involve underestimated particle emissions as well. Furthermore, estimating long-term particle exposure needs the simulations to be done also for seasons with less photochemical activity, in which the role of traffic emissions may be even more highlighted. The results of this study denote only a lower limit of the contribution of traffic to local aerosol levels due to the coarse grid resolution and due to the selection of the simulation period during which the NPF processes are dominating the particle formation.

Code availability. The model code is publicly available at https://github.com/bnmurphy/PMCAMx-UF/

Author contributions. MD, IR, MO, SNP, TR, and JVN designed the research. HK performed the measurements. HK and MO analyzed the measurement data. MO and DP updated the emission inventory. MO ran the simulations. MO, IR and MD analyzed the simulation data. MO prepared the paper with contributions from all co-authors.

Competing interests. The authors declare that they have no conflict of interest.

Acknowledgements. We thank CSC for computational resources. We also thank the authors of the measurement station observation data downloaded from the EBAS and SmartSMEAR databases. Harri Portin and Anu Kousa from the Helsinki Region Environmental Services Authority (HSY) as well as the HSY's AQ measurement team are acknowledged for their valuable work related to the data quality control and measurements at the Mäkelänkatu supersite. This study has been funded by Finnish Cultural Foundation, by the Academy of Finland through the ACCC Flagship (grant no. 337551), and by Tekes (grant no. 2883/31/2015), HSY, and Pegasor Oy through the Cityzer project.

References

Adams, P. and Seinfeld, J.: Predicting global aerosol size distributions in general circulation models, J. Geophys. Res.-Atmos., 107, 4370, https://doi.org/10.1029/2001JD001010, 2002.

Ahlm, L., Julin, J., Fountoukis, C., Pandis, S. N., and Riipinen, I.: Particle number concentrations over Europe in 2030: the role of emissions and new particle formation, Atmos. Chem. Phys., 13, 10 271–10 283, https://doi.org/10.5194/acp-13-10271-2013, 2013.

Alanen, J., Isotalo, M., Kuittinen, N., Simonen, P., Martikainen, S., Kuuluvainen, H., Honkanen, M., Lehtoranta, K., Nyyssönen, S., Vesala, H., Timonen, H., Aurela, M., Keskinen, J., and Rönkkö, T.: Physical Characteristics of Particle Emissions from a Medium Speed Ship Engine Fueled with Natural Gas and Low-Sulfur Liquid Fuels, Environ. Sci. Technol., 54, 5376–5384, https://doi.org/10.1021/acs.est.9b06460, 2020.

Awad, O. I., Ma, X., Kamil, M., Ali, O. M., Zhang, Z., and Shuai, S.: Particulate emissions from gasoline direct injection engines: A review of how current emission regulations are being met by automobile manufacturers, Sci. Total Environ., 718, 137 302, https://doi.org/https://doi.org/10.1016/j.scitotenv.2020.137302, 2020.

Baranizadeh, E., Murphy, B. N., Julin, J., Falahat, S., Reddington, C. L., Arola, A., Ahlm, L., Mikkonen, S., Fountoukis, C., Patoulias, D., Minikin, A., Hamburger, T., Laaksonen, A., Pandis, S. N., Vehkamäki, H., Lehtinen, K. E. J., and Riipinen, I.: Implementation of state-of-the-art ternary new-particle formation scheme to the regional chemical transport model PMCAMx-UF in Europe, Geosci. Model Dev., 9, 2741–2754, https://doi.org/10.5194/gmd-9-2741-2016, 2016.

Barreira, L. M. F., Helin, A., Aurela, M., Teinilä, K., Friman, M., Kangas, L., Niemi, J. V., Portin, H., Kousa, A., Pirjola, L., Rönkkö, T., Saarikoski, S., and Timonen, H.: In-depth characterization of submicron particulate matter inter-annual variations at a street canyon site in northern Europe, Atmos. Chem. Phys., 21, 6297–6314, https://doi.org/10.5194/acp-21-6297-2021, 2021.

CIESIN: Center for International Earth Science Information Network, Columbia University, NASA Socioeconomic Data and Applications Center (SEDAC): Gridded Population of the World, Version 4 (GPWv4): Population Count, Revision 11, https://doi.org/10.7927/H4JW8BX5, last access: 27 Feb 2021, 2018.

Denier van der Gon, H. A. C., Visschedijk, A. J. H., Johansson, C., Hedberg Larsson, E., Harrison, R., and Beddows, D.: Size-resolved pan European anthropogenic particle number inventory, EUCAARI Deliverable report D141 (available on request from EUCAARI project office), 2009.

DieselNet: https://dieselnet.com, last access: 4 Apr 2021, 2021.

EMEP: Centre on Emission Inventories and Projections (CEIP): Officially reported emission data, last access: 2 October 2021, available at: https://www.ceip.at/, 2021.

European Environment Agency: National emissions reported to the UNFCCC and to the EU Greenhouse Gas Monitoring Mechanism - dataset, last access: 1 June 2021, available at: https://www.eea.europa.eu/data-and-maps, 2021.

Eurostat: https://ec.europa.eu/eurostat, last access: 24 Mar 2021, 2021.

Fountoukis, C., Riipinen, I., Denier van der Gon, H. A. C., Charalampidis, P. E., Pilinis, C., Wiedensohler, A., O'Dowd, C., Putaud, J. P., Moerman, M., and Pandis, S. N.: Simulating ultrafine particle formation in Europe using a regional CTM: contribution of primary emissions versus secondary formation to aerosol number concentrations, Atmos. Chem. Phys., 12, 8663–8677, https://doi.org/10.5194/acp-12-8663-2012, 2012.

Giechaskiel, B., Mamakos, A., Andersson, J., Dilara, P., Martini, G., Schindler, W., and Bergmann, A.: Measurement of Automotive Nonvolatile Particle Number Emissions within the European Legislative Framework: A Review, Aerosol Sci. Tech., 46, 719–749, https://doi.org/10.1080/02786826.2012.661103, 2012.

Hao, Y., Deng, S., Yang, Y., Song, W., Tong, H., and Qiu, Z.: Chemical Composition of Particulate Matter from Traffic Emissions in a Road Tunnel in Xi'an, China, Aerosol Air Qual. Res., 19, 234–246, https://doi.org/10.4209/aaqr.2018.04.0131, 2019.

Hietikko, R., Kuuluvainen, H., Harrison, R. M., Portin, H., Timonen, H., Niemi, J. V., and Rönkkö, T.: Diurnal variation of nanocluster aerosol concentrations and emission factors in a street canyon, Atmos. Environ., 189, 98–106, https://doi.org/10.1016/j.atmosenv.2018.06.031, 2018.

ICRP: Human Respiratory Tract Model for Radiological Protection. ICRP Publication 66. Ann. ICRP 24 (1-3), 1994.

Järvi, L., Hannuniemi, H., Hussein, T., Junninen, H., Aalto, P. P., Hillamo, R., Mäkelä, T., Keronen, P., Siivola, E., Vesala, T., and Kulmala, M.: The urban measurement station SMEAR III: Continuous monitoring of air pollution and surface–atmosphere interactions in Helsinki, Finland, Boreal Environ. Res., 14 (suppl. A), 86–109, http://www.borenv.net/BER/archive/ber14A.htm#086, 2009.

Julin, J., Murphy, B. N., Patoulias, D., Fountoukis, C., Olenius, T., Pandis, S. N., and Riipinen, I.: Impacts of Future European Emission Reductions on Aerosol Particle Number Concentrations Accounting for Effects of Ammonia, Amines, and Organic Species, Environ. Sci. Technol., 52, 692–700, https://doi.org/10.1021/acs.est.7b05122, 2018.

Jung, J., Adams, P. J., and Pandis, S. N.: Simulating the size distribution and chemical composition of ultrafine particles during nucleation events, Atmos. Environ., 40, 2248–2259, https://doi.org/10.1016/j.atmosenv.2005.09.082, 2006.

Jung, J., Fountoukis, C., Adams, P. J., and Pandis, S. N.: Simulation of in situ ultrafine particle formation in the eastern United States using PMCAMx-UF, J. Geophys. Res.-Atmos., 115, https://doi.org/10.1029/2009JD012313, 2010.

Kangasluoma, J., Cai, R., Jiang, J., Deng, C., Stolzenburg, D., Ahonen, L. R., Chan, T., Fu, Y., Kim, C., Laurila, T. M., Zhou, Y., Dada, L., Sulo, J., Flagan, R. C., Kulmala, M., Petäjä, T., and Lehtipalo, K.: Overview of measurements and current instrumentation for 1–10 nm aerosol particle number size distributions, J. Aerosol Sci., 148, 105 584, https://doi.org/10.1016/j.jaerosci.2020.105584, 2020.

Kerminen, V.-M., Chen, X., Vakkari, V., Petäjä, T., Kulmala, M., and Bianchi, F.: Atmospheric new particle formation and growth: review of field observations, Environ. Res. Lett., 13, 103 003, https://doi.org/10.1088/1748-9326/aadf3c, 2018.

Keskinen, J. and Rönkkö, T.: Can real-world diesel exhaust particle size distribution be reproduced in the laboratory? A critical review, J. Air Waste Manage., 60, 1245–1255, https://doi.org/10.3155/1047-3289.60.10.1245, 2010.

Kittelson, D., Watts, W., Johnson, J., Thorne, C., Higham, C., Payne, M., Goodier, S., Warrens, C., Preston, H., Zink, U., Pickles, D., Goersmann, C., Twigg, M., Walker, A., and Boddy, R.: Effect of fuel and lube oil sulfur on the performance of a diesel exhaust gas continuously regenerating trap, Environ. Sci. Technol., 42, 9276–9282, https://doi.org/10.1021/es703270j, 2008.

Kontkanen, J., Deng, C., Fu, Y., Dada, L., Zhou, Y., Cai, J., Daellenbach, K. R., Hakala, S., Kokkonen, T. V., Lin, Z., Liu, Y., Wang, Y., Yan, C., Petäjä, T., Jiang, J., Kulmala, M., and Paasonen, P.: Size-resolved particle number emissions in Beijing determined from measured particle size distributions, Atmos. Chem. Physics, 20, 11 329–11 348, https://doi.org/10.5194/acp-20-11329-2020, 2020.

Kostenidou, E., Martinez-Valiente, A., R'Mili, B., Marques, B., Temime-Roussel, B., Durand, A., André, M., Liu, Y., Louis, C., Vansevenant, B., Ferry, D., Laffon, C., Parent, P., and D'Anna, B.: Technical note: Emission factors, chemical composition, and morphology of particles emitted from Euro 5 diesel and gasoline light-duty vehicles during transient cycles, Atmos. Chem. Phys., 21, 4779–4796, https://doi.org/10.5194/acp-21-4779-2021, 2021.

Kulmala, M., Asmi, A., Lappalainen, H. K., Baltensperger, U., Brenguier, J.-L., Facchini, M. C., Hansson, H.-C., Hov, Ø., O'Dowd, C. D., Pöschl, U., Wiedensohler, A., Boers, R., Boucher, O., de Leeuw, G., Denier van der Gon, H. A. C., Feichter, J., Krejci, R., Laj, P.,

Lihavainen, H., Lohmann, U., McFiggans, G., Mentel, T., Pilinis, C., Riipinen, I., Schulz, M., Stohl, A., Swietlicki, E., Vignati, E., Alves, C., Amann, M., Ammann, M., Arabas, S., Artaxo, P., Baars, H., Beddows, D. C. S., Bergström, R., Beukes, J. P., Bilde, M., Burkhart, J. F., Canonaco, F., Clegg, S. L., Coe, H., Crumeyrolle, S., D'Anna, B., Decesari, S., Gilardoni, S., Fischer, M., Fjaeraa, A. M., Fountoukis, C., George, C., Gomes, L., Halloran, P., Hamburger, T., Harrison, R. M., Herrmann, H., Hoffmann, T., Hoose, C., Hu, M., Hyvärinen, A., Hõrrak, U., Iinuma, Y., Iversen, T., Josipovic, M., Kanakidou, M., Kiendler-Scharr, A., Kirkevåg, A., Kiss, G., Klimont, Z., Kolmonen, P., Komppula, M., Kristjánsson, J.-E., Laakso, L., Laaksonen, A., Labonnote, L., Lanz, V. A., Lehtinen, K. E. J., Rizzo, L. V., Makkonen, R., Manninen, H. E., McMeeking, G., Merikanto, J., Minikin, A., Mirme, S., Morgan, W. T., Nemitz, E., O'Donnell, D., Panwar, T. S., Pawlowska, H., Petzold, A., Pienaar, J. J., Pio, C., Plass-Duelmer, C., Prévôt, A. S. H., Pryor, S., Reddington, C. L., Roberts, G., Rosenfeld, D., Schwarz, J., Seland, Ø., Sellegri, K., Shen, X. J., Shiraiwa, M., Siebert, H., Sierau, B., Simpson, D., Sun, J. Y., Topping, D., Tunved, P., Vaattovaara, P., Vakkari, V., Veefkind, J. P., Visschedijk, A., Vuollekoski, H., Vuolo, R., Wehner, B., Wildt, J., Woodward, S., Worsnop, D. R., van Zadelhoff, G.-J., Zardini, A. A., Zhang, K., van Zyl, P. G., Kerminen, V.-M., S Carslaw, K., and Pandis, S. N.: General overview: European Integrated project on Aerosol Cloud Climate and Air Quality interactions (EUCAARI) – integrating aerosol research from nano to global scales, Atmos. Chem. Phys., 11, 13 061–13 143, https://doi.org/10.5194/acp-11-13061-2011, 2011.

Kumar, P., Morawska, L., Birmili, W., Paasonen, P., Hu, M., Kulmala, M., Harrison, R. M., Norford, L., and Britter, R.: Ultrafine particles in cities, Environ. Int., 66, 1–10, https://doi.org/10.1016/j.envint.2014.01.013, 2014.

Kuuluvainen, H., Poikkimäki, M., Järvinen, A., Kuula, J., Irjala, M., Maso, M. D., Keskinen, J., Timonen, H., Niemi, J. V., and Rönkkö, T.: Vertical profiles of lung deposited surface area concentration of particulate matter measured with a drone in a street canyon, Environ. Pollut., 241, 96–105, https://doi.org/10.1016/j.envpol.2018.04.100, 2018.

Kuuluvainen, H., Karjalainen, P., Saukko, E., Ovaska, T., Sirviö, K., Honkanen, M., Olin, M., Niemi, S., Keskinen, J., and Rönkkö, T.: Nonvolatile ultrafine particles observed to form trimodal size distributions in non-road diesel engine exhaust, Aerosol Sci. Tech., 54, 1345–1358, https://doi.org/10.1080/02786826.2020.1783432, 2020.

Lintusaari, H. et al.: Non-volatile particle concentrations in a street canyon environment, manuscript in preparation.

Luoma, K., Niemi, J. V., Aurela, M., Fung, P. L., Helin, A., Hussein, T., Kangas, L., Kousa, A., Rönkkö, T., Timonen, H., Virkkula, A., and Petäjä, T.: Spatiotemporal variation and trends in equivalent black carbon in the Helsinki metropolitan area in Finland, Atmos. Chem. Phys., 21, 1173–1189, https://doi.org/10.5194/acp-21-1173-2021, 2021.

Maher, B. A., Ahmed, I. A. M., Karloukovski, V., MacLaren, D. A., Foulds, P. G., Allsop, D., Mann, D. M. A., Torres-Jardón, R., and Calderon-Garciduenas, L.: Magnetite pollution nanoparticles in the human brain, P. Natl. Acad. Sci. USA, 113, 10 797–10 801, https://doi.org/10.1073/pnas.1605941113, 2016.

Maricq, M., Chase, R., Xu, N., and Laing, P.: The effects of the catalytic converter and fuel sulfur level on motor vehicle particulate matter emissions: Light duty diesel vehicles, Environ. Sci. Technol., 36, 283–289, https://doi.org/10.1021/es010962l, 2002.

Mathis, U., Ristimäki, J., Mohr, M., Keskinen, J., Ntziachristos, L., Samaras, Z., and Mikkanen, P.: Sampling conditions for the measurement of nucleation mode particles in the exhaust of a diesel vehicle, Aerosol Sci. Tech., 38, 1149–1160, https://doi.org/10.1080/027868290891497, 2004.

McGrath, M. J., Olenius, T., Ortega, I. K., Loukonen, V., Paasonen, P., Kurtén, T., Kulmala, M., and Vehkamäki, H.: Atmospheric Cluster Dynamics Code: a flexible method for solution of the birth-death equations, Atmos. Chem. Phys., 12, 2345–2355, https://doi.org/10.5194/acp-12-2345-2012, 2012.

Oberdörster, G., Sharp, Z., Atudorei, V., Elder, A., Gelein, R., Kreyling, W., and Cox, C.: Translocation of Inhaled Ultrafine Particles to the Brain, Inhal. Toxicol., 16, 437–445, https://doi.org/10.1080/08958370490439597, 2004.

Okuljar, M., Kuuluvainen, H., Kontkanen, J., Garmash, O., Olin, M., Niemi, J. V., Timonen, H., Kangasluoma, J., Tham, Y. J., Baalbaki, R., Sipilä, M., Salo, L., Lintusaari, H., Portin, H., Teinilä, K., Aurela, M., Dal Maso, M., Rönkkö, T., Petäjä, T., and Paasonen, P.: Measurement report: The influence of traffic and new particle formation on the size distribution of 1–800 nm particles in Helsinki – a street canyon and an urban background station comparison, Atmos. Chem. Phys., 21, 9931–9953, https://doi.org/10.5194/acp-21-9931-2021, 2021.

Olenius, T., Kupiainen-Määttä, O., Ortega, I. K., Kurtén, T., and Vehkamäki, H.: Free energy barrier in the growth of sulfuric acid–ammonia and sulfuric acid–dimethylamine clusters, J. Chem. Phys., 139, 084 312, https://doi.org/10.1063/1.4819024, 2013.

Olin, M.: Dieselpakokaasun hiukkaspäästöjen muodostumisprosessin simulointi, M.Sc. thesis, Tampere University of Technology, Tampere, Finland, http://urn.fi/URN:NBN:fi:tty-201312191517, 2013.

Olin, M., Anttila, T., and Dal Maso, M.: Using a combined power law and log-normal distribution model to simulate particle formation and growth in a mobile aerosol chamber, Atmos. Chem. Phys., 16, 7067–7090, https://doi.org/10.5194/acp-16-7067-2016, 2016.

Olin, M., Alanen, J., Palmroth, M. R. T., Rönkkö, T., and Dal Maso, M.: Inversely modeling homogeneous $H_2SO_4-H_2O$ nucleation rate in exhaust-related conditions, Atmos. Chem. Phys., 19, 6367–6388, https://doi.org/10.5194/acp-19-6367-2019, 2019.

Olin, M., Kuuluvainen, H., Aurela, M., Kalliokoski, J., Kuittinen, N., Isotalo, M., Timonen, H. J., Niemi, J. V., Rönkkö, T., and Dal Maso, M.: Traffic-originated nanocluster emission exceeds H_2SO_4-driven photochemical new particle formation in an urban area, Atmos. Chem. Phys., 20, 1–13, https://doi.org/10.5194/acp-20-1-2020, 2020.

Paasonen, P., Kupiainen, K., Klimont, Z., Visschedijk, A., Denier van der Gon, H. A. C., and Amann, M.: Continental anthropogenic primary particle number emissions, Atmos. Chem. Phys., 16, 6823–6840, https://doi.org/10.5194/acp-16-6823-2016, 2016.

Patoulias, D., Fountoukis, C., Riipinen, I., Asmi, A., Kulmala, M., and Pandis, S. N.: Simulation of the size-composition distribution of atmospheric nanoparticles over Europe, Atmos. Chem. Phys., 18, 13 639–13 654, https://doi.org/10.5194/acp-18-13639-2018, 2018.

Pirjola, L., Kuuluvainen, H., Timonen, H., Saarikoski, S., Teinilä, K., Salo, L., Datta, A., Simonen, P., Karjalainen, P., Kulmala, K., and Rönkkö, T.: Potential of renewable fuel to reduce diesel exhaust particle emissions, Appl. Energ., 254, 113 636, https://doi.org/https://doi.org/10.1016/j.apenergy.2019.113636, 2019.

Rönkkö, T. and Timonen, H.: Overview of sources and characteristics of nanoparticles in urban traffic-influenced areas, J. Alzheimers Dis., 72, 15–28, https://doi.org/10.3233/JAD-190170, 2019.

Rönkkö, T., Virtanen, A., Vaaraslahti, K., Keskinen, J., Pirjola, L., and Lappi, M.: Effect of dilution conditions and driving parameters on nucleation mode particles in diesel exhaust: Laboratory and on-road study, Atmos. Environ., 40, 2893–2901, https://doi.org/10.1016/j.atmosenv.2006.01.002, 2006.

Rönkkö, T., Kuuluvainen, H., Karjalainen, P., Keskinen, J., Hillamo, R., Niemi, J. V., Pirjola, L., Timonen, H. J., Saarikoski, S., Saukko, E., Järvinen, A., Silvennoinen, H., Rostedt, A., Olin, M., Yli-Ojanperä, J., Nousiainen, P., Kousa, A., and Dal Maso, M.: Traffic is a major source of atmospheric nanocluster aerosol, P. Natl. Acad. Sci. USA, 114, 7549–7554, https://doi.org/10.1073/pnas.1700830114, 2017.

Saha, P. K., Robinson, E. S., Shah, R. U., Zimmerman, N., Apte, J. S., Robinson, A. L., and Presto, A. A.: Reduced Ultrafine Particle Concentration in Urban Air: Changes in Nucleation and Anthropogenic Emissions, Environ. Sci. Technol., 52, 6798–6806, https://doi.org/10.1021/acs.est.8b00910, 2018.

Shi, J. P., Evans, D. E., Khan, A., and Harrison, R. M.: Sources and concentration of nanoparticles (<10nm diameter) in the urban atmosphere, Atmos. Environ., 35, 1193–1202, https://doi.org/10.1016/S1352-2310(00)00418-0, 2001.

Vanhanen, J., Mikkilä, J., Lehtipalo, K., Sipilä, M., Manninen, H. E., Siivola, E., Petäjä, T., and Kulmala, M.: Particle size magnifier for nano-CN detection, Aerosol Sci. Tech., 45, 533–542, https://doi.org/10.1080/02786826.2010.547889, 2011.

Vehkamäki, H., Kulmala, M., Napari, I., Lehtinen, K., Timmreck, C., Noppel, M., and Laaksonen, A.: An improved parameterization for sulfuric acid-water nucleation rates for tropospheric and stratospheric conditions, J. Geophys. Res.-Atmos., 107, 4622, https://doi.org/10.1029/2002JD002184, 2002.

Vouitsis, I., Ntziachristos, L., and Samaras, Z.: Methodology for the quantification of road transport PM emissions, using emission factors or profiles, TRANSPHORM Deliverable D1.1.2, http://transphorm.nilu.no/Portals/51/Documents/Deliverables/NewDeliverables/D1.1.2_updated.pdf, 2013.

Wihersaari, H., Pirjola, L., Karjalainen, P., Saukko, E., Kuuluvainen, H., Kulmala, K., Keskinen, J., and Rönkkö, T.: Particulate emissions of a modern diesel passenger car under laboratory and real-world transient driving conditions, Environ. Pollut., 265, 114 948, https://doi.org/https://doi.org/10.1016/j.envpol.2020.114948, 2020.

1 Trimodal fit equation for emission factor particle size distribution

Emission factor particle size distribution (EFPSD) was fitted to a trimodal distribution with the equation

$$\frac{\mathrm{d}n}{\mathrm{d}\log D_\mathrm{p}} = \left.\frac{\mathrm{d}n}{\mathrm{d}\log D_\mathrm{p}}\right|_\mathrm{power\,law} + \left.\frac{\mathrm{d}n}{\mathrm{d}\log D_\mathrm{p}}\right|_\mathrm{nucleation} + \left.\frac{\mathrm{d}n}{\mathrm{d}\log D_\mathrm{p}}\right|_\mathrm{soot} \tag{S1}$$

where n denotes the emission factor of the particle number belonging to a mode. The first term is expressed with the equation (Olin et al., 2016)

$$\left.\frac{\mathrm{d}n}{\mathrm{d}\log D_\mathrm{p}}\right|_\mathrm{power\,law} = \begin{cases} n\left(\frac{D_\mathrm{p}}{D_2}\right)^\alpha \beta, & D_1 \le D_\mathrm{p} \le D_2 \\ 0, & \mathrm{otherwise} \end{cases} \tag{S2}$$

where β is a scaling function

$$\beta\left(\alpha, \frac{D_1}{D_2}\right) = \begin{cases} \dfrac{\alpha \ln 10}{1-\left(\frac{D_1}{D_2}\right)^\alpha}, & \alpha \neq 0 \\ \dfrac{-\ln 10}{\ln\left(\frac{D_1}{D_2}\right)}, & \alpha = 0 \end{cases} \tag{S3}$$

and α, D_1, and D_2 are the slope parameter and the diameters of the smallest and largest particles of the mode, respectively. The latter two terms are expressed with the equation

$$\left.\frac{\mathrm{d}n}{\mathrm{d}\log D_\mathrm{p}}\right|_\mathrm{nucleation/soot} = \frac{n \ln 10}{\sqrt{2\pi}\ln \mathrm{GSD}} \exp\left[-\frac{\ln^2(D_\mathrm{p}/\mathrm{CMD})}{2\ln^2 \mathrm{GSD}}\right] \tag{S4}$$

where CMD and GSD are the count median diameter and geometric standard deviation of the mode, respectively. The numerical values of the parameters from the fitting are shown in Table 1.

2 Description of the CFD-simulations used to determine chemical composition of the emitted particles

Chemical composition of particles emitted by road traffic was determined using the results from the CFD-simulations by Olin (2013). They consist of a situation where a Euro III bus is driving at a speed of 40 km/h with the engine power of 40 % of the maximum. The situation has been extracted from chasing experiments performed by Rönkkö et al. (2006).

As a Euro III-vehicle, the bus did not have a DPF and it used a diesel fuel having the sulfur content of 50 ppm, which has been the upper limit of the automotive fuel in the EU between years 2004 and 2009.

The simulations were performed using a commercial Ansys Fluent CFD-software with user-defined functions for aerosol dynamics modelling. The CFD-software simulates the flow field (momentum, velocities in 3 dimensions, temperature, and transport of gaseous species) of the bus driving situation including the exhaust flow from the tailpipe. The aerosol model simulates nucleation, condensation, coagulation, deposition, and diffusion of particles emitted directly from the tailpipe and of particles formed from the emitted gaseous precursors after releasing from the tailpipe. The CFD-software also handles the transport of aerosol and connects the aerosol model with temperature and with the concentrations of gaseous species.

Particles were assumed to consist of sulfuric acid (H_2SO_4), water (H_2O), tetracosane ($C_{24}H_{50}$), and soot. Nucleation was modelled as binary H_2SO_4-H_2O nucleation and the nucleation rate was obtained from classical nucleation theory with a correction factor. Condensation modelling included condensation of emitted gases (H_2SO_4, H_2O, and $C_{24}H_{50}$) on emitted soot particles or on particles formed via nucleation. The concentrations of H_2SO_4 and H_2O in the raw exhaust were estimated from fuel and oil sulfur contents and engine parameters. Soot mode properties were obtained from the data measured 10 m behind the bus by chasing. The correction factor for nucleation rate was obtained inversely using measured nucleation mode concentration, i.e., by matching the simulated concentration with the measured one. Particle sizes, instead, were matched with the measured ones using a correction factor for the $C_{24}H_{50}$ concentration, representing the fraction of hydrocarbons which are able to condense on the particles in question.

According to the simulations, particles reached their final sizes (nucleation mode CMD$\sim$10 nm, soot mode CMD$\sim$60 nm) about 5 m behind the bus, but their compositions much earlier. The nucleation mode composition 10 m behind the bus was 11.4 % for H_2SO_4, 25.1 % for H_2O, and 63.5 % for $C_{24}H_{50}$. The soot mode composition was 6.2 % for H_2SO_4, 2.9 % for H_2O, 24.1 % for $C_{24}H_{50}$, and 66.8 % for soot. These (without H_2O) were used as the mass fractions of sulfate (SO_4), primary organic aerosol (POA), and black carbon (BC).

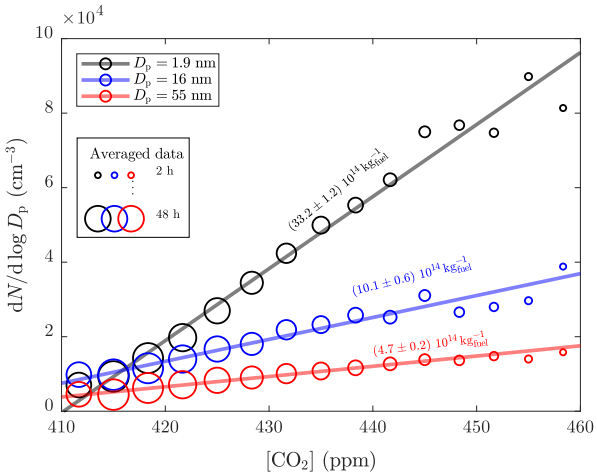

Figure S1. Examples of determining emission factors bin-by-bin for three different particle size bins, similarly to the method by Olin et al. (2020). Size-binned particle number concentration data ($\mathrm{d}N/\mathrm{d}\log D_\mathrm{p}$) are averaged within CO_2 concentration ($[CO_2]$) bins (circle diameters represent the amount of data used in the averaging). Linear fitting (using the circle diameters as weighting factor) is performed over the averaged data (separately for all 28 measured size bins). The slopes of the linear fits converted to kilograms of fuel combusted are marked in the figure.

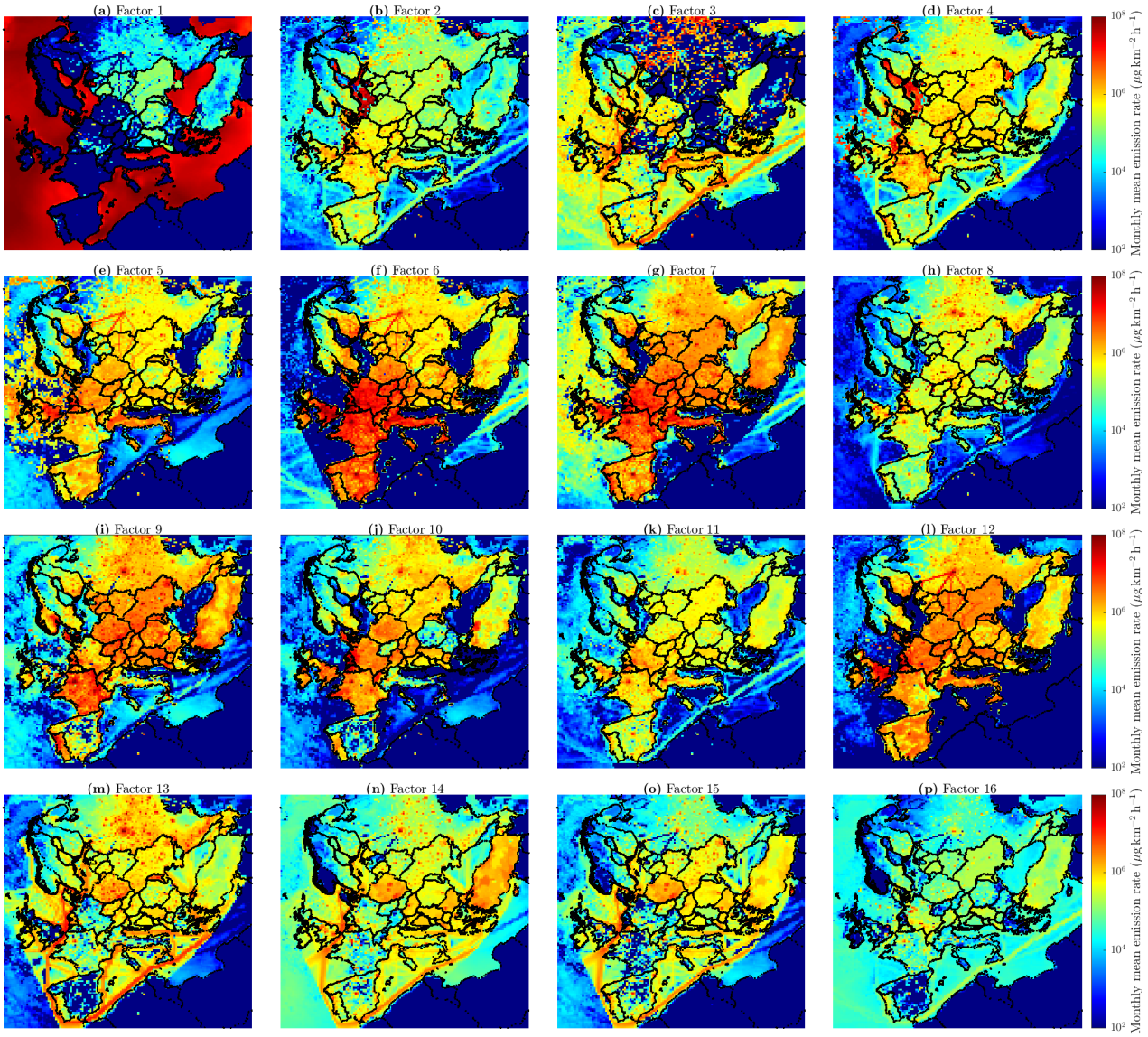

Figure S2. Monthly means of the particle ~~number~~ mass emission rates of all PMF factors (**a**–**p**).

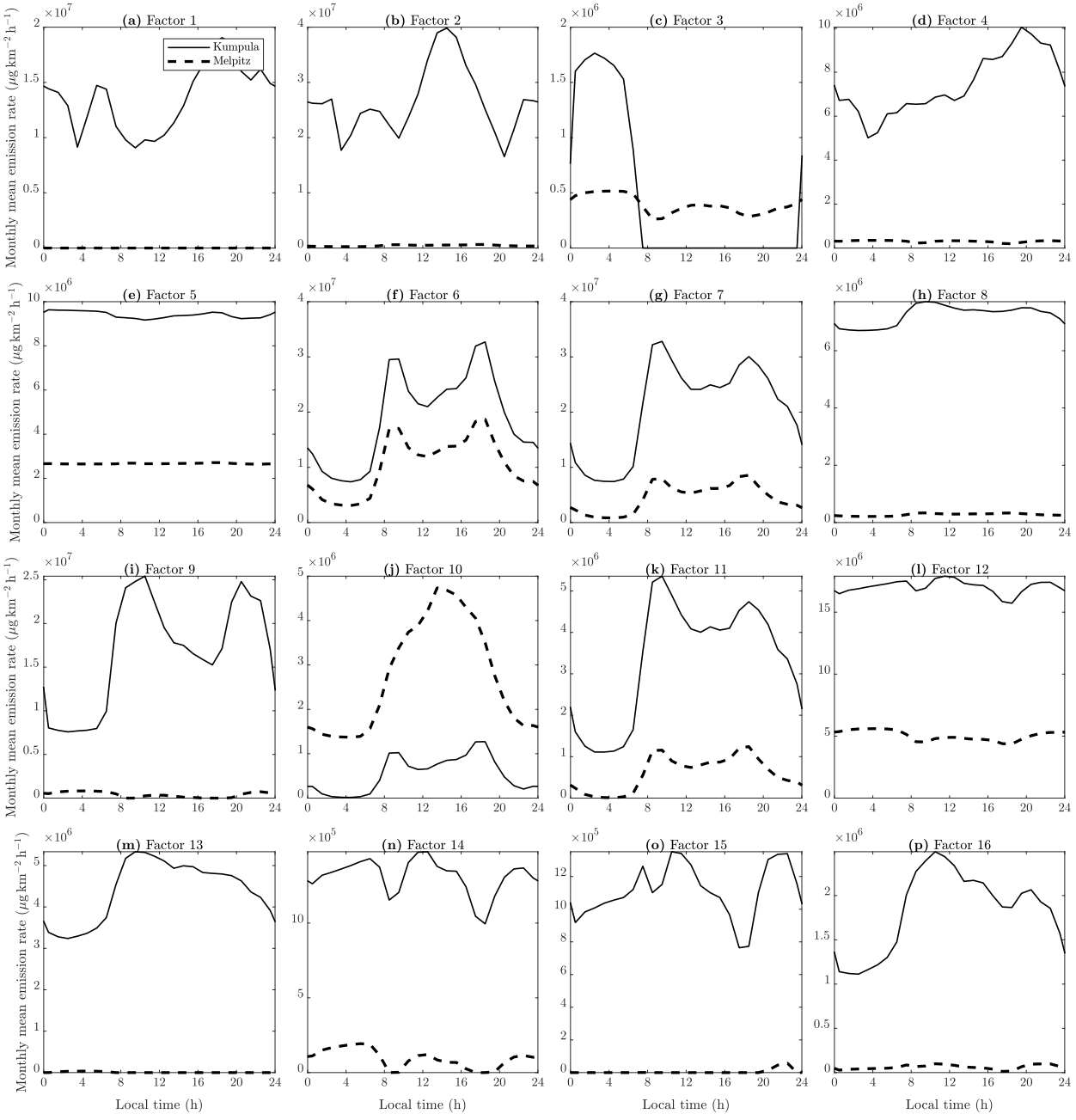

Figure S3. Monthly mean diurnal variations of the particle ~~number~~ mass emission rates in Kumpula/Mäkelänkatu, Finland, and Melpitz, Germany, of all PMF factors (**a**–**p**).

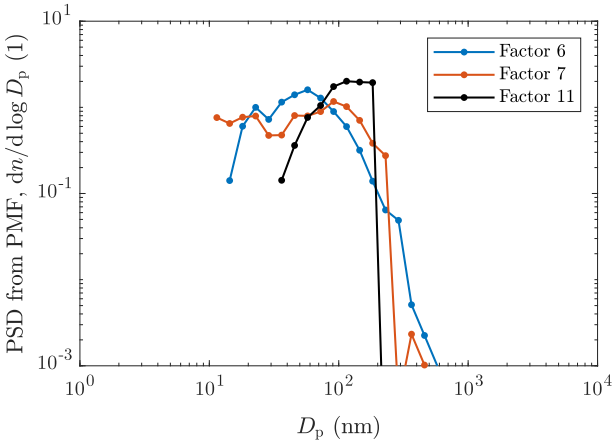

Figure S4. Particle size distributions obtained from PMF factors 6, 7, and 11.

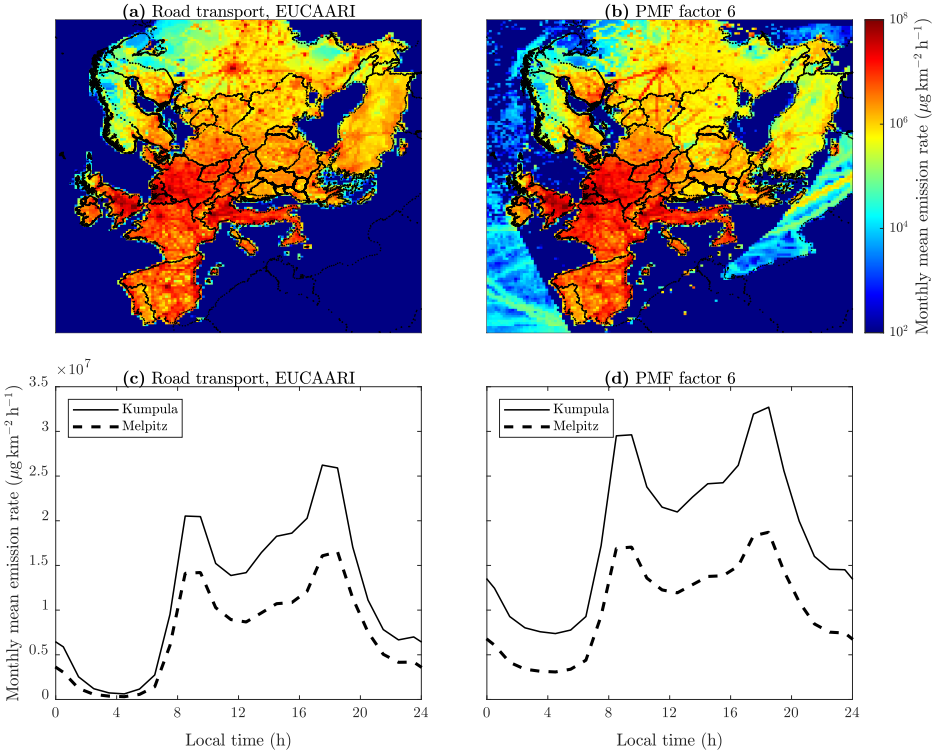

Figure S5. Monthly means of the particle mass emission rates (**a**,**c**) from the road transport-related source in the original EUCAARI inventory and (**b**,**d**) from PMF factor 6 (**a**,**b**) as maps and (**c**,**d**) as diurnal variations in Kumpula/Mäkelänkatu, Finland, and Melpitz, Germany.

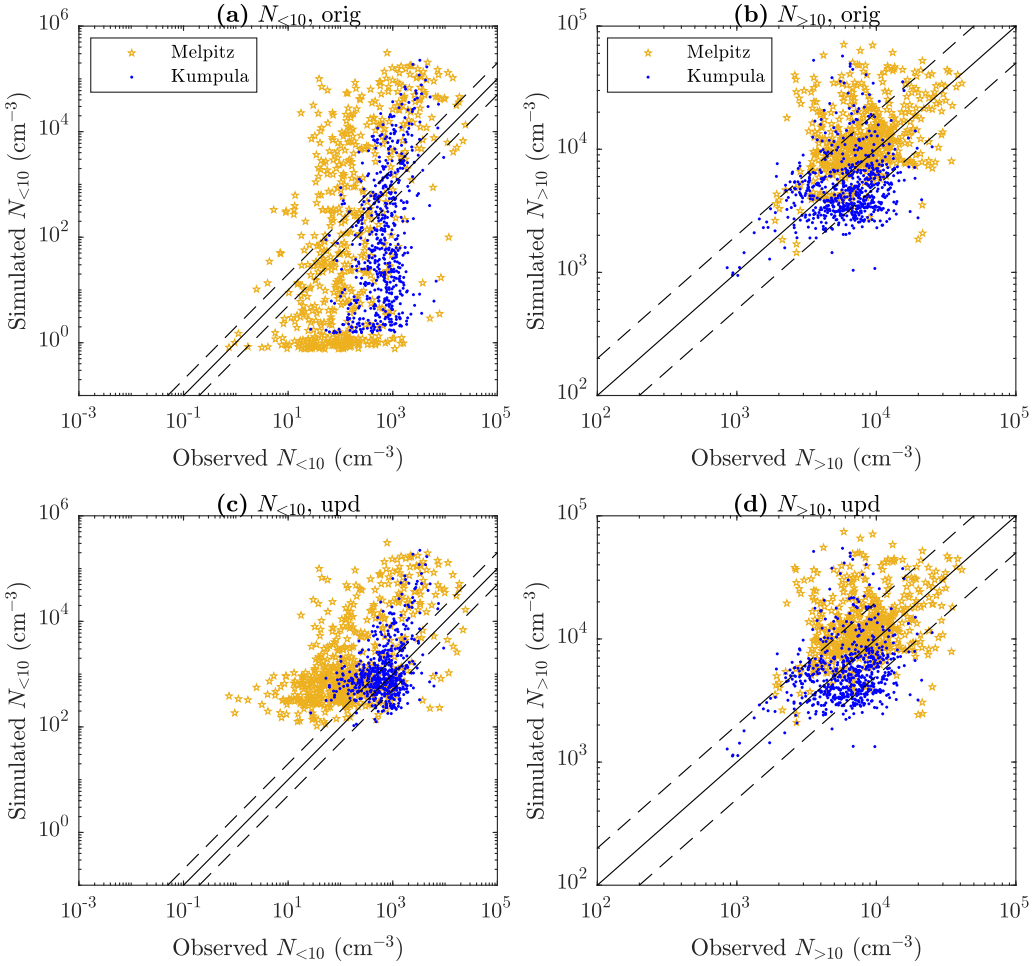

Figure S6. Simulated versus observed number concentrations of particles (**a**, **c**) smaller than 10 nm ($N_{<10}$) and (**b**, **d**) larger than 10 nm ($N_{>10}$) at the stations with the highest traffic influences (Melpitz and Kumpula) with (**a**, **b**) the original and (**c**, **d**) updated emission inventory. All data correspond to hourly means for May 2008. The solid diagonal lines represent 1:1 lines and the dashed ones 1:2 and 2:1 lines.

Table S1. Statistics for grid cell-separated ratios of monthly means of concentrations on the surface-level simulated with the updated and with the original emission inventory. The bold values highlight the particle size ranges experiencing the greatest effects due to updating the inventory.

	$\frac{N_{\mathrm{NCA}}^{\mathrm{upd}}}{N_{\mathrm{NCA}}^{\mathrm{orig}}}$	$\frac{N_{<10}^{\mathrm{upd}}}{N_{<10}^{\mathrm{orig}}}$	$\frac{N_{7-20}^{\mathrm{upd}}}{N_{7-20}^{\mathrm{orig}}}$	$\frac{N_{<23}^{\mathrm{upd}}}{N_{<23}^{\mathrm{orig}}}$	$\frac{N_{<100}^{\mathrm{upd}}}{N_{<100}^{\mathrm{orig}}}$	$\frac{N_{\mathrm{tot}}^{\mathrm{upd}}}{N_{\mathrm{tot}}^{\mathrm{orig}}}$
Mean	**1.113**	1.060	1.019	1.029	1.011	1.009
Population-weighted mean	1.100	1.053	**1.096**	1.034	1.023	1.022
Median	0.9996	1.001	**1.007**	1.0004	1.001	1.002
Population-weighted median	1.004	1.004	**1.043**	1.006	1.006	1.006

References

Olin, M.: Dieselpakokaasun hiukkaspäästöjen muodostumisprosessin simulointi, M.Sc. thesis, Tampere University of Technology, Tampere, Finland, http://urn.fi/URN:NBN:fi:tty-201312191517, 2013.

Olin, M., Anttila, T., and Dal Maso, M.: Using a combined power law and log-normal distribution model to simulate particle formation and growth in a mobile aerosol chamber, Atmos. Chem. Phys., 16, 7067–7090, https://doi.org/10.5194/acp-16-7067-2016, 2016.

Olin, M., Kuuluvainen, H., Aurela, M., Kalliokoski, J., Kuittinen, N., Isotalo, M., Timonen, H. J., Niemi, J. V., Rönkkö, T., and Dal Maso, M.: Traffic-originated nanocluster emission exceeds H_2SO_4-driven photochemical new particle formation in an urban area, Atmos. Chem. Phys., 20, 1–13, https://doi.org/10.5194/acp-20-1-2020, 2020.

Rönkkö, T., Virtanen, A., Vaaraslahti, K., Keskinen, J., Pirjola, L., and Lappi, M.: Effect of dilution conditions and driving parameters on nucleation mode particles in diesel exhaust: Laboratory and on-road study, Atmos. Environ., 40, 2893–2901, https://doi.org/10.1016/j.atmosenv.2006.01.002, 2006.